

## Robin–Robin domain decomposition methods for the steady-state Stokes–Darcy system with the Beavers–Joseph interface condition

Yanzhao Cao · Max Gunzburger · Xiaoming He · Xiaoming Wang

Received: 1 January 2010 / Revised: 5 December 2010 / Published online: 1 March 2011  
© Springer-Verlag 2011

**Abstract** Domain decomposition methods for solving the coupled Stokes–Darcy system with the Beavers–Joseph interface condition are proposed and analyzed. Robin boundary conditions are used to decouple the Stokes and Darcy parts of the system. Then, parallel and serial domain decomposition methods are constructed based on the two decoupled sub-problems. Convergence of the two methods is demonstrated and the results of computational experiments are presented to illustrate the convergence.

**Mathematics Subject Classification (2010)** 65M55 · 65M12 · 65M15 · 65M60 · 35M10 · 35Q35 · 76D07 · 76S05

---

This work is supported in part by the CMG program of the National Science Foundation under grant numbers DMS-0620035 (for MG, XH, and XW) and DMS-0914554 (for YC).

---

Y. Cao  
Department of Mathematics and Statistics, Auburn University, Auburn, AL 36830, USA  
e-mail: yzc0009@auburn.edu

M. Gunzburger · X. He  
Department of Scientific Computing, Florida State University, Tallahassee, FL 32306-4120, USA  
e-mail: gunzburg@fsu.edu

X. He (✉)  
Department of Mathematics and Statistics, Missouri University of Science and Technology,  
Rolla, MO 65409, USA  
e-mail: hex@mst.edu

X. Wang  
Department of Mathematics, Florida State University, Tallahassee, FL 32306, USA  
e-mail: wxm@math.fsu.edu

## 1 Introduction

The Stokes–Darcy model arises in many applications such as groundwater system in karst aquifers, interaction between surface and subsurface flows, industrial filtrations, petroleum extraction, and spontaneous combustion of coal stockpiles. This model describes the free flow of a liquid by the Stokes equation and the confined flow in a porous media by the Darcy equation; the two flows are coupled through interface conditions. For the problems mentioned, the resulting coupled Stokes–Darcy model has higher fidelity than either the Darcy or Stokes systems on their own. However, coupling the two constituent models leads to a very complex system. Most of previous works on the Stokes–Darcy system use the Beavers–Joseph–Saffman (BJS) [45,47,61] interface conditions or even further simplification because well-posedness can be demonstrated in a fairly straightforward manner. However, the BJS condition ignores certain contributions made by the flow in the porous media flow to the coupling of the two models; the ignored contributions may be important in some applications such as karst aquifers. The more physically faithful Beavers–Joseph (BJ) [9] interface condition is more accurate because it fully accounts for the contributions of the two flows in the coupling of the two models.

It is true for some cases that the contribution of the Darcy flow in tangential direction is heuristically much smaller than that of Stokes flow on the interface and hence the Beavers–Joseph–Saffman simplification can be used. However, we are not aware of any rigorous proof on this validity starting from the original Beavers–Joseph interface boundary condition. There are related theoretical works by Chen et al. [23] using the Brinkman–Stokes model as the starting point and periodicity in the horizontal (along the interface) direction. They demonstrated that the Beavers–Joseph interface boundary condition is more accurate than the Beavers–Joseph–Saffman interface boundary condition or its further simplifications. The error is not necessarily small for all parameters and it could be of order 1 for the lower values of the hydraulic conductivity/permeability/porosity.

The major reason why most previous works did not use the BJ condition is that the well posedness of the Stokes–Darcy model with BJ condition had not been demonstrated. However, recently, this problem was resolved in [19,20,23,44] if the primary formulation is used for the Darcy part. For the steady Stokes–Darcy model with the BJ condition, it is proved that the model is well posed if the exchange coefficient  $\alpha$  introduced in (2.7) is sufficiently small.

Several methods have been developed to numerically solve the Stokes–Darcy problem, including coupled finite element methods [4,7,18,19,21,24,34,35,49,60,65], domain decomposition methods [25,28–33,43,46], Lagrange multiplier methods [6,40,50], multi-grid methods [5,17,54], discontinuous Galerkin methods [22,26,41,48,58,59], mortar discretization [12,36–38] and boundary integral methods [13,64]. Many other methods have been developed to solve the Darcy–Stokes(–Brinkman) and other similar models; see [3,8,10–12,16,15,27,42,52,53,55,56,62,63,66,68,69] and the reference cited therein. Among these methods, the domain decomposition method [1,14,39,51,57,67], which can be traced back to [2], is more natural than others because the problem domain naturally consists of two different subdomains and because parallel computation is facilitated; see, e.g., [25] for the BJS condition

and [28–33,43,46] for simplified BJS conditions. In this article, we will extend the previous work in [25] to Robin-type domain decomposition methods for the steady Stokes–Darcy system with BJ interface condition. The BJ condition was first obtained through experiment in [9] and thus reflects the real world problems more precisely.

The rest of paper is organized as follows. In Sect. 2, we introduce the Stokes–Darcy system with the Beavers–Joseph interface condition. In Sect. 3, the system is decoupled by using Robin interface conditions. In Sect. 4, parallel and serial domain decomposition methods are proposed. In Sects. 5 and 6, we analyze the convergence of the domain decomposition methods. Finally, in Sect. 7, we present some numerical results that illustrate the convergence of the domain decomposition methods and show their features.

### 2 Steady Stokes–Darcy model with Beavers–Joseph interface condition

We consider the coupled Stokes–Darcy system on a bounded domain  $\Omega = \Omega_D \cup \Omega_S \subset \mathbb{R}^d$ , ( $d = 2, 3$ ); see Fig. 1. In the porous media region  $\Omega_D$ , the flow is governed by the Darcy system

$$\vec{u}_D = -\mathbb{K}\nabla\phi_D, \tag{2.1}$$

$$\nabla \cdot \vec{u}_D = f_D. \tag{2.2}$$

Here,  $\vec{u}_D$  is the fluid discharge rate in the porous media,  $\mathbb{K}$  is the hydraulic conductivity tensor,  $f_D$  is a sink/source term, and  $\phi_D$  is the hydraulic head defined as  $z + \frac{p_D}{\rho g}$ , where  $p_D$  denotes the dynamic pressure,  $z$  the height,  $\rho$  the density, and  $g$  the gravitational acceleration. In this article, we assume the media in  $\Omega_D$  is homogeneous isotropic so that  $\mathbb{K}$  is a constant scalar matrix. In this article we will consider the following primary formulation for the Darcy system

$$-\nabla \cdot (\mathbb{K}\nabla\phi_D) = f_D.$$

In the fluid region  $\Omega_S$ , the fluid flow is assumed to satisfy the Stokes system

$$-\nabla \cdot \mathbb{T}(\vec{u}_S, p_S) = \vec{f}_S, \tag{2.3}$$

$$\nabla \cdot \vec{u}_S = 0, \tag{2.4}$$

where  $\vec{u}_S$  is the fluid velocity,  $p_S$  is the kinematic pressure,  $\vec{f}_S$  is the external body force,  $\nu$  is the kinematic viscosity of the fluid,  $\mathbb{T}(\vec{u}_S, p_S) = 2\nu\mathbb{D}(\vec{u}_S) - p_S\mathbb{I}$  is the stress tensor, and  $\mathbb{D}(\vec{u}_S) = 1/2(\nabla\vec{u}_S + \nabla^T\vec{u}_S)$  is the deformation tensor.

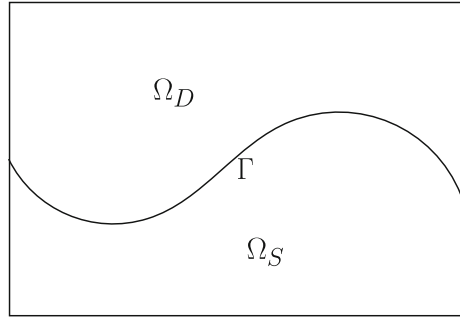
Let  $\Gamma = \overline{\Omega}_D \cap \overline{\Omega}_S$  denote the interface between the fluid and porous media regions. On the interface  $\Gamma$ , we impose the following three interface conditions:

$$\vec{u}_S \cdot \vec{n}_S = -\vec{u}_D \cdot \vec{n}_D, \tag{2.5}$$

$$-\vec{n}_S \cdot (\mathbb{T}(\vec{u}_S, p_S) \cdot \vec{n}_S) = g(\phi_D - z), \tag{2.6}$$

$$-\tau_j \cdot (\mathbb{T}(\vec{u}_S, p_S) \cdot \vec{n}_S) = \frac{\alpha\nu\sqrt{\mathbf{d}}}{\sqrt{\text{trace}(\mathbb{I})}}\tau_j \cdot (\vec{u}_S - \vec{u}_D), \tag{2.7}$$

**Fig. 1** A sketch of the porous media domain  $\Omega_D$ , the free-flow domain  $\Omega_S$ , and the interface  $\Gamma$



where  $\vec{n}_S$  and  $\vec{n}_D$  denote the unit outer normal to the fluid and the porous media regions at the interface  $\Gamma$ , respectively;  $\tau_j (j = 1, \dots, d - 1)$  denote mutually orthogonal unit tangential vectors to the interface  $\Gamma$ , and  $\mathbb{I} = \frac{\mathbb{K}v}{g}$ . The second condition (2.7) is referred to as the Beavers–Joseph (BJ) interface condition [9].

We assume that the hydraulic head  $\phi_D$  and the fluid velocity  $\vec{u}_S$  satisfy homogeneous Dirichlet boundary condition except on  $\Gamma$ , i.e.,  $\phi_D = 0$  on the boundary  $\partial\Omega_D \setminus \Gamma$  and  $\vec{u}_S = 0$  on the boundary  $\partial\Omega_S \setminus \Gamma$ .

The spaces that we utilize are

$$\begin{aligned} X_S &= \{ \vec{v} \in [H^1(\Omega_S)]^d \mid \vec{v} = 0 \text{ on } \partial\Omega_S \setminus \Gamma \}, \\ Q_S &= L^2(\Omega_S), \\ X_D &= \{ \psi \in H^1(\Omega_D) \mid \psi = 0 \text{ on } \partial\Omega_D \setminus \Gamma \}. \end{aligned}$$

For the domain  $D (D = \Omega_S \text{ or } \Omega_D)$ ,  $(\cdot, \cdot)_D$  denotes the  $L^2$  inner product on the domain  $D$ , and  $\langle \cdot, \cdot \rangle$  denotes the  $L^2$  inner product on the interface  $\Gamma$  or the duality pairing between  $(H_{00}^{1/2}(\Gamma))'$  and  $H_{00}^{1/2}(\Gamma)$ .

With these notations, the weak formulation of the coupled Stokes–Darcy problem is given as follows [19,20]: find  $(\vec{u}_S, p_S) \in X_S \times Q_S$  and  $\phi_D \in X_D$  such that

$$\begin{aligned} &a_S(\vec{u}_S, \vec{v}) + b_S(\vec{v}, p_S) + a_D(\phi_D, \psi) + \langle g\phi_D, \vec{v} \cdot \vec{n}_S \rangle - \langle \vec{u}_S \cdot \vec{n}_S, \psi \rangle \\ &+ \frac{\alpha v \sqrt{\mathbf{d}}}{\sqrt{\text{trace}(\mathbb{I})}} \langle P_\tau(\vec{u}_S + \mathbb{K}\nabla\phi_D), P_\tau \vec{v} \rangle \\ &= (f_D, \psi)_{\Omega_D} + (\vec{f}_S, \vec{v})_{\Omega_S} + \langle gz, \vec{v} \cdot \vec{n}_S \rangle \quad \forall \vec{v} \in X_S, \psi \in X_D, \end{aligned} \tag{2.8}$$

$$b_S(\vec{v}, q) = 0, \quad \forall q \in Q_S, \tag{2.9}$$

where the bilinear forms are defined as

$$\begin{aligned} a_D(\phi_D, \psi) &= (\mathbb{K}\nabla\phi_D, \nabla\psi)_{\Omega_D}, \\ a_S(\vec{u}_S, \vec{v}) &= 2\nu(\mathbb{D}(\vec{u}_S), \mathbb{D}(\vec{v}))_{\Omega_S}, \\ b_S(\vec{v}, q) &= -(\nabla \cdot \vec{v}, q)_{\Omega_S}, \end{aligned}$$

and  $P_\tau$  denotes the projection onto the tangent space on  $\Gamma$ , i.e.,

$$P_\tau \vec{u} = \sum_{j=1}^{d-1} (\vec{u} \cdot \tau_j) \tau_j.$$

In this article, we assume that  $\mathbb{K}$  isotropic and  $\alpha$  is small enough. In [20], it is shown that the system of (2.8) and (2.9) is well posed under these two assumptions.

### 3 Robin boundary conditions

In order to solve the coupled Stokes–Darcy problem utilizing a domain decomposition approach, we naturally consider (partial) Robin boundary conditions for the Stokes and the Darcy equations by following the idea in [25].

Let us consider the following Robin condition for the Darcy system: for a given constant  $\gamma_p > 0$  and a given function  $\eta_p$  defined on  $\Gamma$ ,

$$\gamma_p \mathbb{K} \nabla \widehat{\phi}_D \cdot \vec{n}_D + g \widehat{\phi}_D = \eta_p \quad \text{on } \Gamma. \tag{3.10}$$

Then, the corresponding weak formulation for the Darcy system is given by: for  $\eta_p \in L^2(\Gamma)$ , find  $\widehat{\phi}_D \in X_D$  such that

$$a_D(\widehat{\phi}_D, \psi) + \left\langle \frac{g \widehat{\phi}_D}{\gamma_p}, \psi \right\rangle = (f_D, \psi)_{\Omega_D} + \left\langle \frac{\eta_p}{\gamma_p}, \psi \right\rangle \quad \forall \psi \in X_D. \tag{3.11}$$

Similarly, we propose the following two Robin type conditions for the Stokes equations: for a given constant  $\gamma_f > 0$  and given functions  $\eta_f$  and  $\vec{\eta}_{f\tau}$  defined on  $\Gamma$ ,

$$\vec{n}_S \cdot (\mathbb{T}(\vec{u}_S, \widehat{p}_S) \cdot \vec{n}_S) + \gamma_f \widehat{u}_S \cdot \vec{n}_S = \eta_f \quad \text{on } \Gamma, \tag{3.12}$$

$$-P_\tau(\mathbb{T}(\vec{u}_S, \widehat{p}_S) \cdot \vec{n}_S) - \frac{\alpha \nu \sqrt{\mathbf{d}}}{\sqrt{\text{trace}(\mathbb{I})}} P_\tau \widehat{u}_S = \vec{\eta}_{f\tau} \quad \text{on } \Gamma. \tag{3.13}$$

Then, the corresponding weak formulation for the Stokes system is given by: for  $\eta_f, \vec{\eta}_{f\tau} \in L^2(\Gamma)$ , find  $\widehat{u}_S \in X_S$  and  $\widehat{p}_S \in Q_S$  such that

$$\begin{aligned} a_S(\widehat{u}_S, \vec{v}) + b_S(\vec{v}, \widehat{p}_S) + \gamma_f \langle \widehat{u}_S \cdot \vec{n}_S, \vec{v} \cdot \vec{n}_S \rangle + \frac{\alpha \nu \sqrt{\mathbf{d}}}{\sqrt{\text{trace}(\mathbb{I})}} (P_\tau \widehat{u}_S, P_\tau \vec{v}) \\ = (\vec{f}_S, \vec{v})_{\Omega_S} + \langle \eta_f, \vec{v} \cdot \vec{n}_S \rangle - \langle \vec{\eta}_{f\tau}, P_\tau \vec{v} \rangle \quad \forall \vec{v} \in X_S \end{aligned} \tag{3.14}$$

$$b_S(\widehat{u}_S, q) = 0 \quad \forall q \in Q_S. \tag{3.15}$$

We can combine the Stokes and Darcy systems with Robin boundary conditions into one system. Indeed, it is easy to see that if  $\eta_p, \eta_f, \vec{\eta}_{f\tau} \in L^2(\Gamma)$  are given, then,

there exists a unique solution  $(\widehat{\phi}_D, \widehat{u}_f, \widehat{p}_S) \in X_D \times X_S \times Q_S$  such that

$$\begin{aligned}
 & a_S(\widehat{u}_S, \vec{v}) + b_S(\vec{v}, \widehat{p}_S) + a_D(\widehat{\phi}_D, \psi) + \gamma_f \langle \widehat{u}_S \cdot \vec{n}_S, \vec{v} \cdot \vec{n}_S \rangle + \left\langle \frac{g\widehat{\phi}_D}{\gamma_p}, \psi \right\rangle \\
 & + \frac{\alpha v \sqrt{d}}{\sqrt{\text{trace}(\Pi)}} \langle P_\tau \widehat{u}_S, P_\tau \vec{v} \rangle = (f_D, \psi)_{\Omega_D} + (\vec{f}_S, \vec{v})_{\Omega_S} + \langle \eta_f, \vec{v} \cdot \vec{n}_S \rangle \\
 & + \left\langle \frac{\eta_p}{\gamma_p}, \psi \right\rangle - \langle \vec{\eta}_{f\tau}, P_\tau \vec{v} \rangle \quad \forall \psi \in X_D, \vec{v} \in X_S, \tag{3.16}
 \end{aligned}$$

$$b_S(\widehat{u}_S, q) = 0 \quad \forall q \in Q_S. \tag{3.17}$$

Our next step is to show that, for appropriate choices of  $\gamma_f, \gamma_p, \eta_f, \eta_p$ , and  $\vec{\eta}_{f\tau}$ , (smooth) solutions of the Stokes–Darcy system are equivalent to solutions of (3.16), and hence we may solve the latter system instead of the former.

**Lemma 1** *Let  $(\phi_D, \vec{u}_S, p_S)$  be the solution of the coupled Stokes–Darcy system (2.8)–(2.9) and let  $(\widehat{\phi}_D, \widehat{u}_S, \widehat{p}_S)$  be the solution of the decoupled Stokes and Darcy system with Robin boundary conditions (3.16)–(3.17) at the interface. Then,  $(\widehat{\phi}_D, \widehat{u}_S, \widehat{p}_S) = (\phi_D, \vec{u}_S, p_S)$  if and only if  $\gamma_f, \gamma_p, \eta_f, \vec{\eta}_{f\tau}$ , and  $\eta_p$  satisfy the following compatibility conditions:*

$$\eta_p = \gamma_p \widehat{u}_S \cdot \vec{n}_S + g\widehat{\phi}_D, \tag{3.18}$$

$$\eta_f = \gamma_f \widehat{u}_S \cdot \vec{n}_S - g\widehat{\phi}_D + gz, \tag{3.19}$$

$$\vec{\eta}_{f\tau} = \frac{\alpha v \sqrt{d}}{\sqrt{\text{trace}(\Pi)}} P_\tau (\mathbb{K} \nabla \widehat{\phi}_D). \tag{3.20}$$

*Proof* For the necessity, we pick  $\psi = 0$  and  $\vec{v}$  such that  $P_\tau \vec{v} = 0$  in (2.8)–(2.9) and (3.16)–(3.17), then by subtracting (3.16) from (2.8), we get

$$\langle \eta_f - \gamma_f \widehat{u}_S \cdot \vec{n}_S + g\widehat{\phi}_D - gz, \vec{v} \cdot \vec{n}_S \rangle = 0, \quad \forall \vec{v} \in X_S \text{ with } P_\tau \vec{v} = 0$$

which implies (3.19). The necessity of (3.18) and (3.20) can be derived in a similar fashion.

As for the sufficiency, by substituting the compatibility conditions (3.18)–(3.20), we easily see that  $(\widehat{\phi}_D, \widehat{u}_S, \widehat{p}_S)$  solves the coupled Stokes–Darcy system (2.8)–(2.9). Since the solution to the Stokes–Darcy system is unique under the assumption that  $\alpha$  is small enough [20, 44], we have  $(\widehat{\phi}_D, \widehat{u}_S, \widehat{p}_S) = (\phi_D, \vec{u}_S, p_S)$ .

### 4 Robin–Robin domain decomposition methods

#### 4.1 The parallel Robin–Robin domain decomposition method

We propose the following parallel Robin–Robin domain decomposition method for solving the coupled Stokes–Darcy system with the BJ interface condition.

1. Initial values of  $\eta_p^0, \eta_f^0$  and  $\vec{\eta}_{f\tau}^0$  are guessed. They may be taken to be zero.
2. For  $k = 0, 1, 2, \dots$ , independently solve the Stokes and Darcy systems with Robin boundary conditions. More precisely,  $\phi_D^k \in X_D$  is computed from

$$a_D(\phi_D^k, \psi) + \left\langle \frac{g\phi_D^k}{\gamma_p}, \psi \right\rangle = \left\langle \frac{\eta_p^k}{\gamma_p}, \psi \right\rangle + (f_D, \psi)_{\Omega_D} \quad \forall \psi \in X_D$$

and  $\vec{u}_S^k \in X_S$  and  $p_S^k \in Q_S$  are computed from

$$\begin{aligned} a_S(\vec{u}_S^k, \vec{v}) + b_S(\vec{v}, p_S^k) + \gamma_f(\vec{u}_S^k \cdot \vec{n}_S, \vec{v} \cdot \vec{n}_S) + \frac{\alpha v \sqrt{\mathbf{d}}}{\sqrt{\text{trace}(\mathbb{I})}} \langle P_\tau \vec{u}_S^k, P_\tau \vec{v} \rangle \\ = \langle \eta_f^k, \vec{v} \cdot \vec{n}_S \rangle + (\vec{f}_S, \vec{v})_{\Omega_S} - \langle \vec{\eta}_{f\tau}^k, P_\tau \vec{v} \rangle \quad \forall \vec{v} \in X_S, \end{aligned}$$

$$b_S(\vec{u}_S^k, q) = 0 \quad \forall q \in Q_S.$$

3.  $\eta_p^{k+1}, \eta_f^{k+1}$  and  $\vec{\eta}_{f\tau}^{k+1}$  are updated in the following manner:

$$\begin{aligned} \eta_f^{k+1} &= a\eta_p^k + bg\phi_D^k + gz \\ \eta_p^{k+1} &= c\eta_f^k + d\vec{u}_S^k \cdot \vec{n}_S + gz \\ \vec{\eta}_{f\tau}^{k+1} &= \frac{\alpha v \sqrt{\mathbf{d}}}{\sqrt{\text{trace}(\mathbb{I})}} P_\tau(\mathbb{K}\nabla\phi_D^k), \end{aligned}$$

where the coefficients  $a, b, c, d$  are chosen as follows:

$$a = \frac{\gamma_f}{\gamma_p}, \quad b = -1 - a, \quad c = -1, \quad d = \gamma_f + \gamma_p. \tag{4.21}$$

In the special case for which  $\gamma_f = \gamma_p = \gamma$ , we have

$$a = 1 \quad b = -2 \quad c = -1 \quad d = 2\gamma.$$

#### 4.2 The serial Robin–Robin domain decomposition method

Similarly, we have the following serial Robin–Robin domain decomposition method for solving the coupled Stokes–Darcy system with the BJ interface condition.

1. Initial values of  $\eta_p^0, \eta_f^0$  are guessed. They may be taken to be zero.
2. For  $k = 0, 1, 2, \dots$ , solve the Darcy system with Robin boundary condition. More precisely,  $\phi_D^k \in X_D$  is computed from

$$a_D(\phi_D^k, \psi) + \left\langle \frac{g\phi_D^k}{\gamma_p}, \psi \right\rangle = \left\langle \frac{\eta_p^k}{\gamma_p}, \psi \right\rangle + (f_D, \psi)_{\Omega_D} \quad \forall \psi \in X_D;$$

3.  $\vec{\eta}_{f\tau}^k$  is updated in the following manner:

$$\vec{\eta}_{f\tau}^k = \frac{\alpha\nu\sqrt{\mathbf{d}}}{\sqrt{\text{trace}(\mathbb{I})}} P_\tau(\mathbb{K}\nabla\phi_D^k).$$

4. For  $k = 0, 1, 2, \dots$ , independently solve the Stokes and Darcy systems with Robin boundary conditions. More precisely,  $\vec{u}_S^k \in X_S$  and  $p_S^k \in Q_S$  are computed from

$$\begin{aligned} a_S(\vec{u}_S^k, \vec{v}) + b_S(\vec{v}, p_S^k) + \gamma_f \langle \vec{u}_S^k \cdot \vec{n}_S, \vec{v} \cdot \vec{n}_S \rangle + \frac{\alpha\nu\sqrt{\mathbf{d}}}{\sqrt{\text{trace}(\mathbb{I})}} \langle P_\tau \vec{u}_S^k, P_\tau \vec{v} \rangle \\ = \langle \eta_f^k, \vec{v} \cdot \vec{n}_S \rangle + (\vec{f}_S, \vec{v})_{\Omega_S} - \langle \vec{\eta}_{f\tau}^k, P_\tau \vec{v} \rangle \quad \forall \vec{v} \in X_S, \end{aligned}$$

$$b_S(\vec{u}_S^k, q) = 0 \quad \forall q \in Q_S.$$

5.  $\eta_p^{k+1}$  and  $\eta_f^{k+1}$  are updated in the following manner:

$$\begin{aligned} \eta_f^{k+1} &= a\eta_p^k + bg\phi_D^k + gz, \\ \eta_p^{k+1} &= c\eta_f^k + d\vec{u}_S^k \cdot \vec{n}_S + gz. \end{aligned}$$

### 5 Convergence of the parallel Robin–Robin DDM

We follow the elegant energy method proposed in [51] and the arguments in [25] to demonstrate the convergence of the parallel Robin–Robin domain decomposition method for appropriate choice of parameters  $\gamma_p$  and  $\gamma_f$ .

To this end, let  $(\phi_D, \vec{u}_S, p_S)$  denote the solution of the coupled Stokes–Darcy system (2.8)–(2.9). Then, we have that  $(\phi_D, \vec{u}_S, p_S)$  solves the equivalent decoupled system (3.16) with  $\gamma_f, \gamma_p, \eta_p, \eta_f, \vec{\eta}_{f\tau}$  satisfying the compatibility conditions (3.18)–(3.20) with the hats removed. Next, we define the error functions

$$\begin{aligned} \varepsilon_D^k &= \eta_p - \eta_p^k & \varepsilon_S^k &= \eta_f - \eta_f^k & \vec{\varepsilon}_{S\tau}^k &= \vec{\eta}_{f\tau} - \vec{\eta}_{f\tau}^k \\ e_\phi^k &= \phi_D - \phi_D^k & \vec{e}_u^k &= \vec{u}_S - \vec{u}_S^k & e_p^k &= p_S - p_S^k. \end{aligned}$$

Then, the error functions satisfy the following error equations:

$$\gamma_p a_D(e_\phi^k, \psi) + \langle g e_\phi^k, \psi \rangle = \langle \varepsilon_D^k, \psi \rangle \quad \forall \psi \in X_D, \tag{5.22}$$

$$\begin{aligned} a_S(\vec{e}_u^k, \vec{v}) + b_S(\vec{v}, e_p^k) + \gamma_f \langle \vec{e}_u^k \cdot \vec{n}_S, \vec{v} \cdot \vec{n}_S \rangle + \frac{\alpha\nu\sqrt{\mathbf{d}}}{\sqrt{\text{trace}(\mathbb{I})}} \langle P_\tau \vec{e}_u^k, P_\tau \vec{v} \rangle \\ = \langle \varepsilon_S^k, \vec{v} \cdot \vec{n}_S \rangle - \langle \vec{\varepsilon}_{S\tau}^k, P_\tau \vec{v} \rangle \quad \forall \vec{v} \in X_S, \end{aligned} \tag{5.23}$$

$$b_S(\vec{e}_u^k, q) = 0 \quad \forall q \in Q_S, \tag{5.24}$$



and, along the interface  $\Gamma$ ,

$$\varepsilon_S^{k+1} = a\varepsilon_D^k + bge_\phi^k \tag{5.25}$$

$$\varepsilon_D^{k+1} = c\varepsilon_S^k + d\vec{e}_u^k \cdot \vec{n}_S. \tag{5.26}$$

$$\vec{\varepsilon}_{S\tau}^{k+1} = \frac{\alpha\nu\sqrt{\mathbf{d}}}{\sqrt{\text{trace}(\mathbb{I})}} P_\tau(\mathbb{K}\nabla e_\phi^k). \tag{5.27}$$

Equation (5.26) leads to

$$\|\varepsilon_D^{k+1}\|_\Gamma^2 = c^2\|\varepsilon_S^k\|_\Gamma^2 + d^2\|\vec{e}_u^k \cdot \vec{n}_S\|_\Gamma^2 + 2cd\langle\varepsilon_S^k, \vec{e}_u^k \cdot \vec{n}_S\rangle. \tag{5.28}$$

Setting  $\vec{v} = \vec{e}_u^k$  in (5.23), we get

$$\begin{aligned} a_S(\vec{e}_u^k, \vec{e}_u^k) + b_S(\vec{e}_u^k, e_p^k) + \gamma_f\langle\vec{e}_u^k \cdot \vec{n}_S, \vec{e}_u^k \cdot \vec{n}_S\rangle + \frac{\alpha\nu\sqrt{\mathbf{d}}}{\sqrt{\text{trace}(\mathbb{I})}}\langle P_\tau\vec{e}_u^k, P_\tau\vec{e}_u^k\rangle \\ = \langle\varepsilon_S^k, \vec{e}_u^k \cdot \vec{n}_S\rangle - \langle\vec{\varepsilon}_{S\tau}^k, P_\tau\vec{e}_u^k\rangle. \end{aligned}$$

Using (5.24) we have

$$b_S(\vec{e}_u^k, e_p^k) = 0.$$

Hence, by (5.27), we have

$$\begin{aligned} \langle\varepsilon_S^k, \vec{e}_u^k \cdot \vec{n}_S\rangle = a_S(\vec{e}_u^k, \vec{e}_u^k) + \gamma_f\|\vec{e}_u^k \cdot \vec{n}_S\|_\Gamma^2 \\ + \frac{\alpha\nu\sqrt{\mathbf{d}}}{\sqrt{\text{trace}(\mathbb{I})}}\langle P_\tau(\vec{e}_u^k + \mathbb{K}\nabla e_\phi^{k-1}), P_\tau\vec{e}_u^k\rangle, \end{aligned} \tag{5.29}$$

Combining (5.28) and (5.29), we have

$$\begin{aligned} \|\varepsilon_D^{k+1}\|_\Gamma^2 = c^2\|\varepsilon_S^k\|_\Gamma^2 + (d^2 + 2cd\gamma_f)\|\vec{e}_u^k \cdot \vec{n}_S\|_\Gamma^2 + 2cd a_S(\vec{e}_u^k, \vec{e}_u^k) \\ + 2cd \frac{\alpha\nu\sqrt{\mathbf{d}}}{\sqrt{\text{trace}(\mathbb{I})}}\langle P_\tau(\vec{e}_u^k + \mathbb{K}\nabla e_\phi^{k-1}), P_\tau\vec{e}_u^k\rangle. \end{aligned} \tag{5.30}$$

Similarly, (5.25) implies

$$\|\varepsilon_S^{k+1}\|_\Gamma^2 = a^2\|\varepsilon_D^k\|_\Gamma^2 + b^2\|ge_\phi^k\|_\Gamma^2 + 2ab\langle\varepsilon_D^k, ge_\phi^k\rangle.$$

Setting  $\psi = ge_\phi^k$  in (5.22), we have

$$\langle\varepsilon_D^k, ge_\phi^k\rangle = \gamma_p a_D(e_\phi^k, ge_\phi^k) + \langle ge_\phi^k, ge_\phi^k\rangle.$$

Combining the last two equations, we deduce

$$\|\varepsilon_S^{k+1}\|_\Gamma^2 = a^2\|\varepsilon_D^k\|_\Gamma^2 + (b^2 + 2ab)\|ge_\phi^k\|_\Gamma^2 + 2ab\gamma_p g a_D(e_\phi^k, e_\phi^k). \tag{5.31}$$

Substituting (4.21) into (5.30) and (5.31), we have the following result.

**Lemma 2** *The error functions satisfy*

$$\begin{aligned} \|\varepsilon_D^{k+1}\|_\Gamma^2 &= \|\varepsilon_S^k\|_\Gamma^2 + (\gamma_p^2 - \gamma_f^2)\|\vec{e}_u^k \cdot \vec{n}_s\|_\Gamma^2 - 2(\gamma_f + \gamma_p)a_S(\vec{e}_u^k, \vec{e}_u^k) \\ &\quad - 2(\gamma_f + \gamma_p) \frac{\alpha v \sqrt{\mathbf{d}}}{\sqrt{\text{trace}(\mathbb{I})}} \langle P_\tau(\vec{e}_u^k + \mathbb{K}\nabla e_\phi^{k-1}), P_\tau \vec{e}_u^k \rangle, \end{aligned} \tag{5.32}$$

$$\begin{aligned} \|\varepsilon_S^{k+1}\|_\Gamma^2 &= \left(\frac{\gamma_f}{\gamma_p}\right)^2 \|\varepsilon_D^k\|_\Gamma^2 + \left(1 - \left(\frac{\gamma_f}{\gamma_p}\right)^2\right) \|ge_\phi^k\|_\Gamma^2 \\ &\quad - 2\gamma_f \left(1 + \frac{\gamma_f}{\gamma_p}\right) g a_D(e_\phi^k, e_\phi^k). \end{aligned} \tag{5.33}$$

We are now ready to demonstrate the convergence of our parallel Robin–Robin domain decomposition method. The convergence analysis for  $\gamma_f = \gamma_p$  and  $\gamma_f < \gamma_p$  are different and will be treated separately.

*Case 1:*  $\gamma_f = \gamma_p = \gamma$ . In this case, we have

$$\begin{aligned} \|\varepsilon_D^{k+1}\|_\Gamma^2 &= \|\varepsilon_S^k\|_\Gamma^2 - 4\gamma a_S(\vec{e}_u^k, \vec{e}_u^k) - 4\gamma \frac{\alpha v \sqrt{\mathbf{d}}}{\sqrt{\text{trace}(\mathbb{I})}} \langle P_\tau(\vec{e}_u^k + \mathbb{K}\nabla e_\phi^{k-1}), P_\tau \vec{e}_u^k \rangle \\ \|\varepsilon_S^{k+1}\|_\Gamma^2 &= \|\varepsilon_D^k\|_\Gamma^2 - 4\gamma g a_D(e_\phi^k, e_\phi^k). \end{aligned}$$

Adding the two equations and summing over  $k$  from  $k = 1$  to  $N$ , we deduce

$$\begin{aligned} &\|\varepsilon_D^{N+1}\|_\Gamma^2 + \|\varepsilon_S^{N+1}\|_\Gamma^2 \\ &= \|\varepsilon_D^1\|_\Gamma^2 + \|\varepsilon_S^1\|_\Gamma^2 - 4\gamma \sum_{k=1}^N (a_S(\vec{e}_u^k, \vec{e}_u^k) + g a_D(e_\phi^k, e_\phi^k) \\ &\quad + \frac{\alpha v \sqrt{\mathbf{d}}}{\sqrt{\text{trace}(\mathbb{I})}} \langle P_\tau(\vec{e}_u^k + \mathbb{K}\nabla e_\phi^{k-1}), P_\tau \vec{e}_u^k \rangle) \\ &= \|\varepsilon_D^1\|_\Gamma^2 + \|\varepsilon_S^1\|_\Gamma^2 - 4\gamma \sum_{k=1}^N (a_S(\vec{e}_u^k, \vec{e}_u^k) + g a_D(e_\phi^k, e_\phi^k)) \end{aligned}$$

$$\begin{aligned}
 & + \frac{\alpha \nu \sqrt{\mathbf{d}}}{\sqrt{\text{trace}(\mathbb{I})}} \langle P_\tau(\vec{e}_u^k + \mathbb{K} \nabla e_\phi^k), P_\tau \vec{e}_u^k \rangle \\
 & - 4\gamma \sum_{k=1}^N \frac{\alpha \nu \sqrt{\mathbf{d}}}{\sqrt{\text{trace}(\mathbb{I})}} \langle P_\tau(\mathbb{K} \nabla e_\phi^{k-1} - \mathbb{K} \nabla e_\phi^k), P_\tau \vec{e}_u^k \rangle.
 \end{aligned} \tag{5.34}$$

By the coercivity in Lemma 3.2 of [20], when  $\alpha$  is small enough, we have

$$\begin{aligned}
 & a_S(\vec{e}_u^k, \vec{e}_u^k) + g_{AD}(e_\phi^k, e_\phi^k) + \frac{\alpha \nu \sqrt{\mathbf{d}}}{\sqrt{\text{trace}(\mathbb{I})}} \langle P_\tau(\vec{e}_u^k + \mathbb{K} \nabla e_\phi^k), P_\tau \vec{e}_u^k \rangle \\
 & \geq C_1 \left( \|\vec{e}_u^k\|_1^2 + \|e_\phi^k\|_1^2 \right),
 \end{aligned} \tag{5.35}$$

where  $C_1$  depends on  $K$  and  $\nu$  linearly. Since we suppose  $\mathbb{K}$  is isotropic, then  $\mathbb{K} = K\mathbb{I}$  where  $K$  is a constant and  $\mathbb{I}$  is the identity matrix. Since the tangential projection of the gradient to the tangential plane is the tangential derivative, then  $(P_\tau(\mathbb{K} \nabla e_\phi^k))|_\Gamma = K \nabla_\tau(e_\phi^k|_\Gamma)$  where  $\nabla_\tau(e_\phi^k|_\Gamma)$  is the gradient derivative of  $e_\phi^k|_\Gamma$ . Hence, we have  $P_\tau \vec{e}_u^k|_\Gamma \in H_{00}^{1/2}(\Gamma)$  and  $(P_\tau(\mathbb{K} \nabla e_\phi^k))|_\Gamma \in (H_{00}^{1/2}(\Gamma))'$ . Using the Cauchy–Schwarz inequality, the triangle inequality, and trace theorems, we have

$$\begin{aligned}
 & \sum_{k=1}^N \langle P_\tau(\mathbb{K} \nabla e_\phi^{k-1} - \mathbb{K} \nabla e_\phi^k), P_\tau \vec{e}_u^k \rangle \\
 & \geq - \sum_{k=1}^N \|P_\tau(\mathbb{K} \nabla e_\phi^{k-1} - \mathbb{K} \nabla e_\phi^k)\|_{-1/2, \Gamma} \|P_\tau \vec{e}_u^k\|_{1/2, \Gamma} \\
 & \geq - \sum_{k=1}^N \left( \|P_\tau(\mathbb{K} \nabla e_\phi^{k-1})\|_{-1/2, \Gamma} + \|P_\tau(\mathbb{K} \nabla e_\phi^k)\|_{-1/2, \Gamma} \right) \|P_\tau \vec{e}_u^k\|_{1/2, \Gamma} \\
 & \geq -CK \sum_{k=1}^N \left( \|e_\phi^{k-1}\|_1 + \|e_\phi^k\|_1 \right) \|\vec{e}_u^k\|_1 \\
 & \geq -C_2 \sum_{k=0}^N \left( \|\vec{e}_u^k\|_1^2 + \|e_\phi^k\|_1^2 \right),
 \end{aligned} \tag{5.36}$$

where  $C_2$  depends on  $K$  linearly. Hence, plugging (5.35) and (5.36) into (5.34), we get

$$\begin{aligned}
 0 & \leq \|\varepsilon_D^{N+1}\|_\Gamma^2 + \|\varepsilon_S^{N+1}\|_\Gamma^2 \\
 & \leq \|\varepsilon_D^1\|_\Gamma^2 + \|\varepsilon_S^1\|_\Gamma^2 + 4\gamma C_1 \left( \|\vec{e}_u^0\|_1^2 + \|e_\phi^0\|_1^2 \right) \\
 & \quad - 4\gamma \left( C_1 - C_2 \frac{\alpha \nu \sqrt{\mathbf{d}}}{\sqrt{\text{trace}(\mathbb{I})}} \right) \sum_{k=0}^N \left( \|\vec{e}_u^k\|_1^2 + \|e_\phi^k\|_1^2 \right)
 \end{aligned}$$

Hence, for any positive integer  $N$ ,

$$\begin{aligned}
 & 4\gamma \left( C_1 - C_2 \frac{\alpha\nu\sqrt{\mathbf{d}}}{\sqrt{\text{trace}(\mathbb{I})}} \right) \sum_{k=0}^N \left( \|\vec{e}_u^k\|_1^2 + \|e_\phi^k\|_1^2 \right) \\
 & \leq \left( \|\varepsilon_D^1\|_\Gamma^2 + \|\varepsilon_S^1\|_\Gamma^2 \right) + 4\gamma C_1 \left( \|\vec{e}_u^0\|_1^2 + \|e_\phi^0\|_1^2 \right).
 \end{aligned}$$

If  $\alpha$  is small enough such that

$$C_1 - C_2 \frac{\alpha\nu\sqrt{\mathbf{d}}}{\sqrt{\text{trace}(\mathbb{I})}} > 0, \tag{5.37}$$

then  $\vec{e}_u^k$  and  $e_\phi^k$  tend to zero in  $(H^1(\Omega_S))^d$  and  $H^1(\Omega_D)$ , respectively. The convergence of  $e_\phi^k$  together with the error equation (5.22) implies the convergence of  $\varepsilon_D^k$  in  $H^{-\frac{1}{2}}(\Gamma)$ . Combining the convergence of  $\varepsilon_D^k$  and  $e_\phi^k$  and the error equation on the interface (5.25), we deduce the convergence of  $\varepsilon_S^k$  in  $H^{-\frac{1}{2}}(\Gamma)$ . Combining the convergence of  $e_\phi^k$  and the error equation on the interface (5.27), we deduce the convergence of  $\vec{e}_{S\tau}^k$  in  $H^{-\frac{1}{2}}(\Gamma)$ . The convergence of the pressure then follows from the inf–sup condition and (5.23). Hence we have proved the following theorem.

**Theorem 1** *Assume  $\gamma_f = \gamma_p = \gamma$ ,  $\mathbb{K}$  is isotropic, and  $\alpha$  is small enough such that (5.35) and (5.37) are satisfied. Then,*

$$\begin{aligned}
 & \phi_D^k \xrightarrow{X_D} \phi_D \quad \vec{u}_S^k \xrightarrow{X_S} \vec{u}_S \quad p_f^k \xrightarrow{Q_S} p_S, \\
 & \eta_p^k \xrightarrow{H^{-\frac{1}{2}}(\Gamma)} \gamma \vec{u}_S \cdot \vec{n}_S + g\phi_D = -\gamma \mathbb{K} \nabla \phi_D \cdot \vec{n}_D + g\phi_D, \\
 & \eta_f^k \xrightarrow{H^{-\frac{1}{2}}(\Gamma)} \gamma \vec{u}_S \cdot \vec{n}_S - g\phi_D = \vec{n}_S \cdot (\mathbb{T}(\vec{u}_S, p_S) \cdot \vec{n}_S) + \gamma \vec{u}_S \cdot \vec{n}_S, \\
 & \vec{\eta}_{f\tau}^k \xrightarrow{H^{-\frac{1}{2}}(\Gamma)} \frac{\alpha\nu\sqrt{\mathbf{d}}}{\sqrt{\text{trace}(\mathbb{I})}} P_\tau \mathbb{K} \nabla \phi_D.
 \end{aligned}$$

Case 2:  $\gamma_f < \gamma_p$ . Multiplying (5.32) by  $\frac{\gamma_f}{\gamma_p}$  and adding it to (5.33), we get

$$\begin{aligned}
 & \frac{\gamma_f}{\gamma_p} \|\varepsilon_D^{k+1}\|_\Gamma^2 + \|\varepsilon_S^{k+1}\|_\Gamma^2 \\
 & = \left( \frac{\gamma_f}{\gamma_p} \right)^2 \|\varepsilon_D^k\|_\Gamma^2 + \frac{\gamma_f}{\gamma_p} \|\varepsilon_S^k\|_\Gamma^2 + \frac{\gamma_f}{\gamma_p} (\gamma_p^2 - \gamma_f^2) \|\vec{e}_u^k \cdot \vec{n}_S\|_\Gamma^2 - 2\frac{\gamma_f}{\gamma_p} (\gamma_f + \gamma_p) \\
 & \quad \times a_S(\vec{e}_u^k, \vec{e}_u^k) - 2\frac{\gamma_f}{\gamma_p} (\gamma_f + \gamma_p) \frac{\alpha\nu\sqrt{\mathbf{d}}}{\sqrt{\text{trace}(\mathbb{I})}} \langle P_\tau(\vec{e}_u^k + \mathbb{K} \nabla e_\phi^{k-1}), P_\tau \vec{e}_u^k \rangle
 \end{aligned}$$

$$\begin{aligned}
 & + \left( 1 - \left( \frac{\gamma_f}{\gamma_p} \right)^2 \right) \|g e_\phi^k\|_\Gamma^2 - 2\gamma_f \left( 1 + \frac{\gamma_f}{\gamma_p} \right) g a_D(e_\phi^k, e_\phi^k) \\
 = & \left( \frac{\gamma_f}{\gamma_p} \right)^2 \|\varepsilon_D^k\|_\Gamma^2 + \frac{\gamma_f}{\gamma_p} \|\varepsilon_S^k\|_\Gamma^2 + \frac{\gamma_f}{\gamma_p} (\gamma_p^2 - \gamma_f^2) \|\vec{e}_u^k \cdot \vec{n}_s\|_\Gamma^2 \\
 & + \left( 1 - \left( \frac{\gamma_f}{\gamma_p} \right)^2 \right) \|g e_\phi^k\|_\Gamma^2 - 2\frac{\gamma_f}{\gamma_p} (\gamma_f + \gamma_p) \left[ a_S(\vec{e}_u^k, \vec{e}_u^k) + g a_D(e_\phi^k, e_\phi^k) \right. \\
 & \left. + \frac{\alpha v \sqrt{\mathbf{d}}}{\sqrt{\text{trace}(\mathbb{II})}} \langle P_\tau(\vec{e}_u^k + \mathbb{K} \nabla e_\phi^{k-1}), P_\tau \vec{e}_u^k \rangle \right].
 \end{aligned}$$

Then summing over  $k$  from  $k = 1$  to  $N$ , we deduce

$$\begin{aligned}
 0 \leq & \frac{\gamma_f}{\gamma_p} \|\varepsilon_D^{N+1}\|_\Gamma^2 + \sum_{k=2}^N \left[ \frac{\gamma_f}{\gamma_p} - \left( \frac{\gamma_f}{\gamma_p} \right)^2 \right] \|\varepsilon_D^k\|_\Gamma^2 + \|\varepsilon_S^{N+1}\|_\Gamma^2 + \sum_{k=2}^N \left[ 1 - \frac{\gamma_f}{\gamma_p} \right] \|\varepsilon_S^k\|_\Gamma^2 \\
 = & \left( \frac{\gamma_f}{\gamma_p} \right)^2 \|\varepsilon_D^1\|_\Gamma^2 + \frac{\gamma_f}{\gamma_p} \|\varepsilon_S^1\|_\Gamma^2 + \frac{\gamma_f}{\gamma_p} (\gamma_p^2 - \gamma_f^2) \sum_{k=1}^N \|\vec{e}_u^k \cdot \vec{n}_s\|_\Gamma^2 \\
 & + \left[ 1 - \left( \frac{\gamma_f}{\gamma_p} \right)^2 \right] \sum_{k=1}^N \|g e_\phi^k\|_\Gamma^2 - 2\frac{\gamma_f}{\gamma_p} (\gamma_f + \gamma_p) \sum_{k=1}^N \left[ a_S(\vec{e}_u^k, \vec{e}_u^k) \right. \\
 & \left. + \frac{\alpha v \sqrt{\mathbf{d}}}{\sqrt{\text{trace}(\mathbb{II})}} \langle P_\tau(\vec{e}_u^k + \mathbb{K} \nabla e_\phi^{k-1}), P_\tau \vec{e}_u^k \rangle + g a_D(e_\phi^k, e_\phi^k) \right] \\
 = & \left( \frac{\gamma_f}{\gamma_p} \right)^2 \|\varepsilon_D^1\|_\Gamma^2 + \frac{\gamma_f}{\gamma_p} \|\varepsilon_S^1\|_\Gamma^2 + \frac{\gamma_f}{\gamma_p} (\gamma_p^2 - \gamma_f^2) \sum_{k=1}^N \|\vec{e}_u^k \cdot \vec{n}_s\|_\Gamma^2 \\
 & + \left[ 1 - \left( \frac{\gamma_f}{\gamma_p} \right)^2 \right] \sum_{k=1}^N \|g e_\phi^k\|_\Gamma^2 - 2\frac{\gamma_f}{\gamma_p} (\gamma_f + \gamma_p) \sum_{k=1}^N \left[ a_S(\vec{e}_u^k, \vec{e}_u^k) \right. \\
 & \left. + \frac{\alpha v \sqrt{\mathbf{d}}}{\sqrt{\text{trace}(\mathbb{II})}} \langle P_\tau(\vec{e}_u^k + \mathbb{K} \nabla e_\phi^k), P_\tau \vec{e}_u^k \rangle + g a_D(e_\phi^k, e_\phi^k) \right] \\
 & - 2\frac{\gamma_f}{\gamma_p} (\gamma_f + \gamma_p) \sum_{k=1}^N \frac{\alpha v \sqrt{\mathbf{d}}}{\sqrt{\text{trace}(\mathbb{II})}} \langle P_\tau(\mathbb{K} \nabla e_\phi^{k-1} - \mathbb{K} \nabla e_\phi^k), P_\tau \vec{e}_u^k \rangle. \tag{5.38}
 \end{aligned}$$

By the trace inequality and the Poincaré inequality, we have

$$\|\vec{e}_u^k \cdot \vec{n}_s\|_\Gamma^2 \leq C_3 \|\vec{e}_u^k\|_1^2, \tag{5.39}$$

$$\|g e_\phi^k\|_\Gamma^2 \leq g^2 C_4 \|e_\phi^k\|_1^2. \tag{5.40}$$

Suppose  $\alpha$  is small enough such that (5.35) is true. Then by (5.35), (5.36), and the above three inequalities, we get

$$\begin{aligned}
 0 &\leq \frac{\gamma_f}{\gamma_p} \|\varepsilon_D^{N+1}\|_\Gamma^2 + \sum_{k=2}^N \left[ \frac{\gamma_f}{\gamma_p} - \left( \frac{\gamma_f}{\gamma_p} \right)^2 \right] \|\varepsilon_D^k\|_\Gamma^2 + \|\varepsilon_S^{N+1}\|_\Gamma^2 + \sum_{k=2}^N \left[ 1 - \frac{\gamma_f}{\gamma_p} \right] \|\varepsilon_S^k\|_\Gamma^2 \\
 &\leq \left( \frac{\gamma_f}{\gamma_p} \right)^2 \|\varepsilon_D^1\|_\Gamma^2 + \frac{\gamma_f}{\gamma_p} \|\varepsilon_S^1\|_\Gamma^2 + \frac{\gamma_f}{\gamma_p} (\gamma_p^2 - \gamma_f^2) C_3 \sum_{k=1}^N \|\vec{e}_u^k\|_1^2 \\
 &\quad + \left[ 1 - \left( \frac{\gamma_f}{\gamma_p} \right)^2 \right] g^2 C_4 \sum_{k=1}^N \|e_\phi^k\|_1^2 + 2 \frac{\gamma_f}{\gamma_p} (\gamma_f + \gamma_p) C_1 \left( \|\vec{e}_u^0\|_1^2 + \|e_\phi^0\|_1^2 \right) \\
 &\quad - 2 \frac{\gamma_f}{\gamma_p} (\gamma_f + \gamma_p) \left( C_1 - C_2 \frac{\alpha v \sqrt{\mathbf{d}}}{\sqrt{\text{trace}(\Pi)}} \right) \sum_{k=0}^N \left( \|\vec{e}_u^k\|_1^2 + \|e_\phi^k\|_1^2 \right). \tag{5.41}
 \end{aligned}$$

Fix any number  $s \in (0, 2)$ . Suppose  $\gamma_f$  and  $\gamma_p$  are chosen such that

$$\begin{aligned}
 \frac{\gamma_f}{\gamma_p} (\gamma_p^2 - \gamma_f^2) C_3 - s \frac{\gamma_f}{\gamma_p} (\gamma_f + \gamma_p) \left( C_1 - C_2 \frac{\alpha v \sqrt{\mathbf{d}}}{\sqrt{\text{trace}(\Pi)}} \right) &\leq 0, \\
 \left[ 1 - \left( \frac{\gamma_f}{\gamma_p} \right)^2 \right] g^2 C_4 - s \frac{\gamma_f}{\gamma_p} (\gamma_f + \gamma_p) \left( C_1 - C_2 \frac{\alpha v \sqrt{\mathbf{d}}}{\Pi} \right) &\leq 0,
 \end{aligned}$$

which are equivalent to

$$\gamma_p - \gamma_f \leq \frac{s \left( C_1 - C_2 \frac{\alpha v \sqrt{\mathbf{d}}}{\sqrt{\text{trace}(\Pi)}} \right)}{C_3}, \tag{5.42}$$

$$\frac{1}{\gamma_f} - \frac{1}{\gamma_p} \leq \frac{s \left( C_1 - C_2 \frac{\alpha v \sqrt{\mathbf{d}}}{\sqrt{\text{trace}(\Pi)}} \right)}{g^2 C_4}. \tag{5.43}$$

Then, we get

$$\begin{aligned}
 0 &\leq \frac{\gamma_f}{\gamma_p} \|\varepsilon_D^{N+1}\|_\Gamma^2 + \sum_{k=2}^N \left[ \frac{\gamma_f}{\gamma_p} - \left( \frac{\gamma_f}{\gamma_p} \right)^2 \right] \|\varepsilon_D^k\|_\Gamma^2 + \|\varepsilon_S^{N+1}\|_\Gamma^2 + \sum_{k=2}^N \left[ 1 - \frac{\gamma_f}{\gamma_p} \right] \|\varepsilon_S^k\|_\Gamma^2 \\
 &\leq \left( \frac{\gamma_f}{\gamma_p} \right)^2 \|\varepsilon_D^1\|_\Gamma^2 + \frac{\gamma_f}{\gamma_p} \|\varepsilon_S^1\|_\Gamma^2 + 2 \frac{\gamma_f}{\gamma_p} (\gamma_f + \gamma_p) C_1 \left( \|\vec{e}_u^0\|_1^2 + \|e_\phi^0\|_1^2 \right) \\
 &\quad - (2 - s) \frac{\gamma_f}{\gamma_p} (\gamma_f + \gamma_p) \left( C_1 - C_2 \frac{\alpha v \sqrt{\mathbf{d}}}{\sqrt{\text{trace}(\Pi)}} \right) \sum_{k=0}^N \left[ \|\vec{e}_u^k\|_1^2 + \|e_\phi^k\|_1^2 \right].
 \end{aligned}$$

With the same argument as the end of the Case 1, we obtain the convergence for Case 2.

Now we derive a geometric convergence rate for Case 2. Similar to (5.35), we still need to assume that  $\alpha$  is small enough such that

$$\begin{aligned}
 & a_S(\vec{e}_u^k, \vec{e}_u^k) + g a_D(e_\phi^{k-1}, e_\phi^{k-1}) + \frac{\alpha v \sqrt{\mathbf{d}}}{\sqrt{\text{trace}(\mathbb{I})}} \langle P_\tau(\vec{e}_u^k + \mathbb{K}\nabla e_\phi^{k-1}), P_\tau \vec{e}_u^k \rangle \\
 & \geq C_1 \left( \|\vec{e}_u^k\|_1^2 + \|e_\phi^{k-1}\|_1^2 \right).
 \end{aligned}
 \tag{5.44}$$

Also, it is easy to see

$$a_D(e_\phi^{k-1}, e_\phi^{k-1}) \leq C_5 \|e_\phi^{k-1}\|_1^2.
 \tag{5.45}$$

where  $C_5$  depends on  $K$ . Plugging (5.33) into (5.32) and using (5.39), (5.40), (5.44), and (5.45), we have

$$\begin{aligned}
 & \|\varepsilon_D^{k+1}\|_\Gamma^2 \\
 & = \left(\frac{\gamma_f}{\gamma_p}\right)^2 \|\varepsilon_D^{k-1}\|_\Gamma^2 + \left(1 - \left(\frac{\gamma_f}{\gamma_p}\right)^2\right) \|g e_\phi^{k-1}\|_\Gamma^2 - 2\gamma_f \left(1 + \frac{\gamma_f}{\gamma_p}\right) g a_D(e_\phi^{k-1}, e_\phi^{k-1}) \\
 & \quad + (\gamma_p^2 - \gamma_f^2) \|\vec{e}_u^k \cdot \vec{n}_S\|_\Gamma^2 - 2(\gamma_f + \gamma_p) a_S(\vec{e}_u^k, \vec{e}_u^k) \\
 & \quad - 2(\gamma_f + \gamma_p) \frac{\alpha v \sqrt{\mathbf{d}}}{\sqrt{\text{trace}(\mathbb{I})}} \langle P_\tau(\vec{e}_u^k + \mathbb{K}\nabla e_\phi^{k-1}), P_\tau \vec{e}_u^k \rangle \\
 & = \left(\frac{\gamma_f}{\gamma_p}\right)^2 \|\varepsilon_D^{k-1}\|_\Gamma^2 + \left(1 - \left(\frac{\gamma_f}{\gamma_p}\right)^2\right) \|g e_\phi^{k-1}\|_\Gamma^2 \\
 & \quad + 2(\gamma_f + \gamma_p) \left(1 - \frac{\gamma_f}{\gamma_p}\right) g a_D(e_\phi^{k-1}, e_\phi^{k-1}) + (\gamma_p^2 - \gamma_f^2) \|\vec{e}_u^k \cdot \vec{n}_S\|_\Gamma^2 \\
 & \quad - 2(\gamma_f + \gamma_p) \left[ a_S(\vec{e}_u^k, \vec{e}_u^k) + g a_D(e_\phi^{k-1}, e_\phi^{k-1}) \right. \\
 & \quad \left. + \frac{\alpha v \sqrt{\mathbf{d}}}{\sqrt{\text{trace}(\mathbb{I})}} \langle P_\tau(\vec{e}_u^k + \mathbb{K}\nabla e_\phi^{k-1}), P_\tau \vec{e}_u^k \rangle \right] \\
 & \leq \left(\frac{\gamma_f}{\gamma_p}\right)^2 \|\varepsilon_D^{k-1}\|_\Gamma^2 + \left(1 - \left(\frac{\gamma_f}{\gamma_p}\right)^2\right) g^2 C_4 \|e_\phi^{k-1}\|_1^2 \\
 & \quad + 2(\gamma_f + \gamma_p) \left(1 - \frac{\gamma_f}{\gamma_p}\right) g C_5 \|e_\phi^{k-1}\|_1^2 + (\gamma_p^2 - \gamma_f^2) C_3 \|\vec{e}_u^k\|_1^2 \\
 & \quad - 2(\gamma_f + \gamma_p) C_1 \left( \|\vec{e}_u^k\|_1^2 + \|e_\phi^{k-1}\|_1^2 \right).
 \end{aligned}
 \tag{5.46}$$

Fix any number  $s \in (0, 2)$ . Suppose  $\gamma_f$  and  $\gamma_p$  are chosen such that

$$\begin{aligned}
 &(\gamma_p^2 - \gamma_f^2)C_3 - s(\gamma_f + \gamma_p)C_1 \leq 0, \\
 &\left[ 1 - \left(\frac{\gamma_f}{\gamma_p}\right)^2 \right] g^2C_4 + 2(\gamma_f + \gamma_p) \left( 1 - \frac{\gamma_f}{\gamma_p} \right) gC_5 - s(\gamma_f + \gamma_p)C_1 \leq 0,
 \end{aligned}$$

which are equivalent to

$$\gamma_p - \gamma_f \leq \frac{sC_1}{C_3}, \tag{5.47}$$

$$\gamma_p - \gamma_f \leq \frac{s\gamma_p^2C_1}{g^2C_4 + 2\gamma_p gC_5}. \tag{5.48}$$

Then, we have

$$\|\varepsilon_D^{k+1}\|_\Gamma^2 + (2 - s)(\gamma_f + \gamma_p)C_1 \left( \|\vec{e}_u^k\|_1^2 + \|e_\phi^{k-1}\|_1^2 \right) \leq \left(\frac{\gamma_f}{\gamma_p}\right)^2 \|\varepsilon_D^{k-1}\|_\Gamma^2.$$

Hence, we get the geometric convergence rate  $\sqrt{\frac{\gamma_f}{\gamma_p}}$  for  $\varepsilon_D^k$ ,  $\vec{e}_u^k$ , and  $e_\phi^k$ . Using (5.22)–(5.27), we obtain the geometric convergence rate  $\sqrt{\frac{\gamma_f}{\gamma_p}}$  for  $\varepsilon_S^k$ ,  $e_p^k$  and  $\vec{e}_{S\tau}^k$ . Hence we have proved the following theorem.

**Theorem 2** *Assume  $\gamma_f < \gamma_p$ ,  $\mathbb{K}$  is isotropic, and  $\alpha$  is small enough such that (5.35) and (5.37) are satisfied. If  $\gamma_f$  and  $\gamma_p$  are close to each other such that (5.42) and (5.43) are true, then,*

$$\begin{aligned}
 &\phi_D^k \xrightarrow{X_D} \phi_D \quad \vec{u}_S^k \xrightarrow{X_S} \vec{u}_S \quad p_f^k \xrightarrow{Q_S} p_S, \\
 &\eta_p^k \xrightarrow{L^2(\Gamma)} \gamma_p \vec{u}_S \cdot \vec{n}_S + g\phi_D = -\gamma_p \mathbb{K} \nabla \phi_D \cdot \vec{n}_D + g\phi_D, \\
 &\eta_f^k \xrightarrow{L^2(\Gamma)} \gamma_f \vec{u}_S \cdot \vec{n}_S - g\phi_D = \vec{n}_S \cdot (\mathbb{T}(\vec{u}_S, p_S) \cdot \vec{n}_S) + \gamma_f \vec{u}_S \cdot \vec{n}_S, \\
 &\vec{\eta}_{f\tau}^k \xrightarrow{H^{-\frac{1}{2}}(\Gamma)} \frac{\alpha v \sqrt{d}}{\sqrt{\text{trace}(\mathbb{T})}} P_\tau \mathbb{K} \nabla \phi_D.
 \end{aligned}$$

Specifically, if  $\gamma_f$  and  $\gamma_p$  are close to each other such that (5.47) and (5.48) are true, then we have geometric convergence rate  $\sqrt{\frac{\gamma_f}{\gamma_p}}$ .

*Remark 1* Even though the Beavers–Joseph constant  $\alpha$  is required to be sufficiently small so that (5.35) and (5.37) are satisfied, the restriction is actually not severe. A straightforward calculation based on (5.35) and (5.37) implies that  $\alpha$  is of order one. Therefore the coefficient on the right-hand-side of (2.7) is formally of the order of  $\frac{v}{\sqrt{\text{trace}(\mathbb{T})}}$  and it would be of the order of  $10^{-2}$  to  $\sqrt{10}$  for practical parameters



$\nu = 10^{-7}$  and  $10^{-6} \leq k \leq 10^{-2}$  in the international system. Hence the right-hand-side of (2.7) is not necessarily small and should not be neglected.

### 6 Convergence of the serial Robin–Robin DDM

In this section, we similarly demonstrate the convergence of the serial Robin–Robin domain decomposition method for appropriate choice of parameters  $\gamma_p$  and  $\gamma_f$ . Most of the notations are the same as those of the previous section. First, the error functions still satisfy (5.22)–(5.26), but (5.27) is changed to be

$$\vec{e}_{S\tau}^k = \frac{\alpha\nu\sqrt{\mathbf{d}}}{\sqrt{\text{trace}(\mathbb{I})}} P_\tau(\mathbb{K}\nabla e_\phi^k). \tag{6.49}$$

With similar arguments for Lemma 2, we get the following lemma.

**Lemma 3** *The error functions satisfy*

$$\begin{aligned} \|\varepsilon_D^{k+1}\|_\Gamma^2 &= \|\varepsilon_S^k\|_\Gamma^2 + (\gamma_p^2 - \gamma_f^2) \|\vec{e}_u^k \cdot \vec{n}_S\|_\Gamma^2 - 2(\gamma_f + \gamma_p) a_S(\vec{e}_u^k, \vec{e}_u^k) \\ &\quad - 2(\gamma_f + \gamma_p) \frac{\alpha\nu\sqrt{\mathbf{d}}}{\sqrt{\text{trace}(\mathbb{I})}} \langle P_\tau(\vec{e}_u^k + \mathbb{K}\nabla e_\phi^k), P_\tau \vec{e}_u^k \rangle, \end{aligned} \tag{6.50}$$

$$\begin{aligned} \|\varepsilon_S^{k+1}\|_\Gamma^2 &= \left(\frac{\gamma_f}{\gamma_p}\right)^2 \|\varepsilon_D^k\|_\Gamma^2 + \left(1 - \left(\frac{\gamma_f}{\gamma_p}\right)^2\right) \|g e_\phi^k\|_\Gamma^2 \\ &\quad - 2\gamma_f \left(1 + \frac{\gamma_f}{\gamma_p}\right) g a_D(e_\phi^k, e_\phi^k). \end{aligned} \tag{6.51}$$

Following the same idea as in the previous section, we are now ready to demonstrate the convergence of our serial Robin–Robin domain decomposition method. Again the convergence analysis for  $\gamma_f = \gamma_p$  and  $\gamma_f < \gamma_p$  will be treated separately.

*Case 1:*  $\gamma_f = \gamma_p = \gamma$ . In this case, we have

$$\begin{aligned} \|\varepsilon_D^{k+1}\|_\Gamma^2 &= \|\varepsilon_S^k\|_\Gamma^2 - 4\gamma a_S(\vec{e}_u^k, \vec{e}_u^k) - 4\gamma \frac{\alpha\nu\sqrt{\mathbf{d}}}{\sqrt{\text{trace}(\mathbb{I})}} \langle P_\tau(\vec{e}_u^k + \mathbb{K}\nabla e_\phi^k), P_\tau \vec{e}_u^k \rangle \\ \|\varepsilon_S^{k+1}\|_\Gamma^2 &= \|\varepsilon_D^k\|_\Gamma^2 - 4\gamma g a_D(e_\phi^k, e_\phi^k). \end{aligned}$$

Adding the two equations and summing over  $k$  from  $k = 0$  to  $N$ , we deduce

$$\begin{aligned} \|\varepsilon_D^{N+1}\|_\Gamma^2 + \|\varepsilon_S^{N+1}\|_\Gamma^2 &= \|\varepsilon_D^0\|_\Gamma^2 + \|\varepsilon_S^0\|_\Gamma^2 - 4\gamma \sum_{k=0}^N (a_S(\vec{e}_u^k, \vec{e}_u^k) + g a_D(e_\phi^k, e_\phi^k)) \\ &\quad + \frac{\alpha\nu\sqrt{\mathbf{d}}}{\sqrt{\text{trace}(\mathbb{I})}} \langle P_\tau(\vec{e}_u^k + \mathbb{K}\nabla e_\phi^k), P_\tau \vec{e}_u^k \rangle. \end{aligned}$$

Suppose  $\alpha$  is small enough such that (5.35) is true. Then,

$$0 \leq \|\varepsilon_D^{N+1}\|_\Gamma^2 + \|\varepsilon_S^{N+1}\|_\Gamma^2 \leq \|\varepsilon_D^0\|_\Gamma^2 + \|\varepsilon_S^0\|_\Gamma^2 - 4\gamma C_1 \sum_{k=0}^N \left( \|\vec{e}_u^k\|_1^2 + \|e_\phi^k\|_1^2 \right)$$

which leads to

$$4\gamma C_1 \sum_{k=0}^N \left( \|\vec{e}_u^k\|_1^2 + \|e_\phi^k\|_1^2 \right) \leq \|\varepsilon_D^0\|_\Gamma^2 + \|\varepsilon_S^0\|_\Gamma^2 \text{ for arbitrary positive integer } N.$$

This implies that  $\vec{e}_u^k$  and  $e_\phi^k$  tend to zero in  $(H^1(\Omega_S))^d$  and  $H^1(\Omega_D)$ , respectively. With the same arguments in the previous section, we obtain the convergence for Case 1 as follows.

**Theorem 3** Assume  $\gamma_f = \gamma_p = \gamma$ ,  $\mathbb{K}$  is isotropic, and  $\alpha$  is small enough such that (5.35) is true. Then,

$$\begin{aligned} \phi_D &\xrightarrow{X_D} \phi_D \quad \vec{u}_S^k \xrightarrow{X_S} \vec{u}_S \quad p_f^k \xrightarrow{Q_S} p_S, \\ \eta_p^k &\xrightarrow{H^{-\frac{1}{2}}(\Gamma)} \gamma \vec{u}_S \cdot \vec{n}_S + g\phi_D = -\gamma \mathbb{K} \nabla \phi_D \cdot \vec{n}_D + g\phi_D, \\ \eta_f^k &\xrightarrow{H^{-\frac{1}{2}}(\Gamma)} \gamma \vec{u}_S \cdot \vec{n}_S - g\phi_D = \vec{n}_S \cdot (\mathbb{T}(\vec{u}_S, p_S) \cdot \vec{n}_S) + \gamma \vec{u}_S \cdot \vec{n}_S, \\ \vec{\eta}_{f\tau}^k &\xrightarrow{H^{-\frac{1}{2}}(\Gamma)} \frac{\alpha v \sqrt{d}}{\sqrt{\text{trace}(\mathbb{I})}} P_\tau \mathbb{K} \nabla \phi_D. \end{aligned}$$

Case 2:  $\gamma_f < \gamma_p$ . Multiplying (6.50) by  $\frac{\gamma_f}{\gamma_p}$  and adding it to (6.51), we get

$$\begin{aligned} &\frac{\gamma_f}{\gamma_p} \|\varepsilon_D^{k+1}\|_\Gamma^2 + \|\varepsilon_S^{k+1}\|_\Gamma^2 \\ &= \left( \frac{\gamma_f}{\gamma_p} \right)^2 \|\varepsilon_D^k\|_\Gamma^2 + \frac{\gamma_f}{\gamma_p} \|\varepsilon_S^k\|_\Gamma^2 + \frac{\gamma_f}{\gamma_p} (\gamma_p^2 - \gamma_f^2) \|\vec{e}_u^k \cdot \vec{n}_S\|_\Gamma^2 \\ &\quad - 2 \frac{\gamma_f}{\gamma_p} (\gamma_f + \gamma_p) a_S (\vec{e}_u^k, \vec{e}_u^k) - 2 \frac{\gamma_f}{\gamma_p} (\gamma_f + \gamma_p) \frac{\alpha v \sqrt{d}}{\sqrt{\text{trace}(\mathbb{I})}} \\ &\quad \times \langle P_\tau (\vec{e}_u^k + \mathbb{K} \nabla e_\phi^k), P_\tau \vec{e}_u^k \rangle + \left[ 1 - \left( \frac{\gamma_f}{\gamma_p} \right)^2 \right] \|g e_\phi^k\|_\Gamma^2 \\ &\quad - 2\gamma_f \left( 1 + \frac{\gamma_f}{\gamma_p} \right) g a_D (e_\phi^k, e_\phi^k) \end{aligned}$$

$$\begin{aligned}
 &= \left(\frac{\gamma_f}{\gamma_p}\right)^2 \|\varepsilon_D^k\|_\Gamma^2 + \frac{\gamma_f}{\gamma_p} \|\varepsilon_S^k\|_\Gamma^2 + \frac{\gamma_f}{\gamma_p} (\gamma_p^2 - \gamma_f^2) \|\vec{e}_u^k \cdot \vec{n}_S\|_\Gamma^2 \\
 &+ \left[1 - \left(\frac{\gamma_f}{\gamma_p}\right)^2\right] \|ge_\phi^k\|_\Gamma^2 - 2\frac{\gamma_f}{\gamma_p} (\gamma_f + \gamma_p) \left[ a_S(\vec{e}_u^k, \vec{e}_u^k) + ga_D(e_\phi^k, e_\phi^k) \right. \\
 &\left. + \frac{\alpha\nu\sqrt{\mathbf{d}}}{\sqrt{\text{trace}(\mathbb{I})}} \langle P_\tau(\vec{e}_u^k + \mathbb{K}\nabla e_\phi^k), P_\tau \vec{e}_u^k \rangle \right]. \tag{6.52}
 \end{aligned}$$

Then summing over  $k$  from  $k = 0$  to  $N$ , we deduce

$$\begin{aligned}
 0 &\leq \frac{\gamma_f}{\gamma_p} \|\varepsilon_D^{N+1}\|_\Gamma^2 + \sum_{k=1}^N \left[ \frac{\gamma_f}{\gamma_p} - \left(\frac{\gamma_f}{\gamma_p}\right)^2 \right] \|\varepsilon_D^k\|_\Gamma^2 + \|\varepsilon_S^{N+1}\|_\Gamma^2 + \sum_{k=1}^N \left[1 - \frac{\gamma_f}{\gamma_p}\right] \|\varepsilon_S^k\|_\Gamma^2 \\
 &= \left(\frac{\gamma_f}{\gamma_p}\right)^2 \|\varepsilon_D^0\|_\Gamma^2 + \frac{\gamma_f}{\gamma_p} \|\varepsilon_S^0\|_\Gamma^2 + \frac{\gamma_f}{\gamma_p} (\gamma_p^2 - \gamma_f^2) \sum_{k=0}^N \|\vec{e}_u^k \cdot \vec{n}_S\|_\Gamma^2 \\
 &+ \left[1 - \left(\frac{\gamma_f}{\gamma_p}\right)^2\right] \sum_{k=0}^N \|ge_\phi^k\|_\Gamma^2 - 2\frac{\gamma_f}{\gamma_p} (\gamma_f + \gamma_p) \sum_{k=0}^N \left[ a_S(\vec{e}_u^k, \vec{e}_u^k) + ga_D(e_\phi^k, e_\phi^k) \right. \\
 &\left. + \frac{\alpha\nu\sqrt{\mathbf{d}}}{\sqrt{\text{trace}(\mathbb{I})}} \langle P_\tau(\vec{e}_u^k + \mathbb{K}\nabla e_\phi^k), P_\tau \vec{e}_u^k \rangle \right]. \tag{6.53}
 \end{aligned}$$

Suppose  $\alpha$  is small enough such that (5.35) is true. Then by (5.35), (5.39), (5.40), and the above inequality we get

$$\begin{aligned}
 0 &\leq \frac{\gamma_f}{\gamma_p} \|\varepsilon_D^{N+1}\|_\Gamma^2 + \sum_{k=1}^N \left[ \frac{\gamma_f}{\gamma_p} - \left(\frac{\gamma_f}{\gamma_p}\right)^2 \right] \|\varepsilon_D^k\|_\Gamma^2 + \|\varepsilon_S^{N+1}\|_\Gamma^2 + \sum_{k=1}^N \left[1 - \frac{\gamma_f}{\gamma_p}\right] \|\varepsilon_S^k\|_\Gamma^2 \\
 &\leq \left(\frac{\gamma_f}{\gamma_p}\right)^2 \|\varepsilon_D^0\|_\Gamma^2 + \frac{\gamma_f}{\gamma_p} \|\varepsilon_S^0\|_\Gamma^2 + \frac{\gamma_f}{\gamma_p} (\gamma_p^2 - \gamma_f^2) C_3 \sum_{k=0}^N \|\vec{e}_u^k\|_\Gamma^2 \\
 &+ \left[1 - \left(\frac{\gamma_f}{\gamma_p}\right)^2\right] g^2 C_4 \sum_{k=0}^N \|e_\phi^k\|_\Gamma^2 - 2\frac{\gamma_f}{\gamma_p} (\gamma_f + \gamma_p) C_1 \sum_{k=0}^N \left[ \|\vec{e}_u^k\|_\Gamma^2 + \|e_\phi^k\|_\Gamma^2 \right].
 \end{aligned}$$

Fix any number  $s \in (0, 2)$ . Suppose  $\gamma_f$  and  $\gamma_p$  are chosen such that

$$\begin{aligned}
 &\frac{\gamma_f}{\gamma_p} (\gamma_p^2 - \gamma_f^2) C_3 - s \frac{\gamma_f}{\gamma_p} (\gamma_f + \gamma_p) C_1 \leq 0, \\
 &\left[1 - \left(\frac{\gamma_f}{\gamma_p}\right)^2\right] g^2 C_4 - s \frac{\gamma_f}{\gamma_p} (\gamma_f + \gamma_p) C_1 \leq 0
 \end{aligned}$$

which are equivalent to

$$\gamma_p - \gamma_f \leq \frac{sC_1}{C_3}, \tag{6.54}$$

$$\frac{1}{\gamma_f} - \frac{1}{\gamma_p} \leq \frac{sC_1}{g^2C_4}. \tag{6.55}$$

Then we get

$$\begin{aligned} 0 &\leq \frac{\gamma_f}{\gamma_p} \|\varepsilon_D^{N+1}\|_\Gamma^2 + \sum_{k=1}^N \left[ \frac{\gamma_f}{\gamma_p} - \left( \frac{\gamma_f}{\gamma_p} \right)^2 \right] \|\varepsilon_D^k\|_\Gamma^2 + \|\varepsilon_S^{N+1}\|_\Gamma^2 + \sum_{k=1}^N \left[ 1 - \frac{\gamma_f}{\gamma_p} \right] \|\varepsilon_S^k\|_\Gamma^2 \\ &= \left( \frac{\gamma_f}{\gamma_p} \right)^2 \|\varepsilon_D^0\|_\Gamma^2 + \frac{\gamma_f}{\gamma_p} \|\varepsilon_S^0\|_\Gamma^2 - (2-s)(\gamma_f + \gamma_p)C_1 \sum_{k=0}^N \left[ \|\vec{e}_u^k\|_1^2 + \|e_\phi^k\|_1^2 \right]. \end{aligned}$$

With similar argument in the previous section, we finish the convergence for Case 2.

Now we derive a geometric convergence rate for Case 2. We still need to assume that  $\alpha$  is small enough such that (5.35) is true; then, substituting (5.35), (5.39), and (5.40) into (6.52) we get

$$\begin{aligned} &\frac{\gamma_f}{\gamma_p} \|\varepsilon_D^{k+1}\|_\Gamma^2 + \|\varepsilon_S^{k+1}\|_\Gamma^2 \\ &\leq \left( \frac{\gamma_f}{\gamma_p} \right)^2 \|\varepsilon_D^k\|_\Gamma^2 + \frac{\gamma_f}{\gamma_p} \|\varepsilon_S^k\|_\Gamma^2 + \left( 1 - \left( \frac{\gamma_f}{\gamma_p} \right)^2 \right) g^2 C_4 \|e_\phi^k\|_1^2 \\ &\quad + \frac{\gamma_f}{\gamma_p} (\gamma_p^2 - \gamma_f^2) C_3 \|\vec{e}_u^k\|_1^2 - 2 \frac{\gamma_f}{\gamma_p} (\gamma_f + \gamma_p) C_1 \left( \|\vec{e}_u^k\|_1^2 + \|e_\phi^k\|_1^2 \right). \end{aligned}$$

Suppose  $\gamma_f$  and  $\gamma_p$  are chosen such that

$$\begin{aligned} &\frac{\gamma_f}{\gamma_p} (\gamma_p^2 - \gamma_f^2) C_3 - s \frac{\gamma_f}{\gamma_p} (\gamma_f + \gamma_p) C_1 \leq 0, \\ &\left[ 1 - \left( \frac{\gamma_f}{\gamma_p} \right)^2 \right] g^2 C_4 - s \frac{\gamma_f}{\gamma_p} (\gamma_f + \gamma_p) C_1 \leq 0 \end{aligned}$$

which are equivalent to

$$\gamma_p - \gamma_f \leq \frac{sC_1}{C_3}, \tag{6.56}$$

$$\frac{1}{\gamma_f} - \frac{1}{\gamma_p} \leq \frac{sC_1}{g^2C_4}. \tag{6.57}$$

Then, we have

$$\begin{aligned} & \left( \frac{\gamma_f}{\gamma_p} \|\varepsilon_D^{k+1}\|_\Gamma^2 + \|\varepsilon_S^{k+1}\|_\Gamma^2 \right) + (2-s) \frac{\gamma_f}{\gamma_p} (\gamma_f + \gamma_p) C_1 \left( \|\vec{e}_u^k\|_1^2 + \|e_\phi^k\|_1^2 \right) \\ & \leq \frac{\gamma_f}{\gamma_p} \left( \frac{\gamma_f}{\gamma_p} \|\varepsilon_D^k\|_\Gamma^2 + \|\varepsilon_S^k\|_\Gamma^2 \right). \end{aligned}$$

Hence, we get the geometric convergence rate  $\sqrt{\frac{\gamma_f}{\gamma_p}}$  for  $\varepsilon_D^k, \varepsilon_S^k, \vec{e}_u^k$ , and  $e_\phi^k$ . Using (5.22)–(5.26) and (6.49), we obtain the geometric convergence rate  $\sqrt{\frac{\gamma_f}{\gamma_p}}$  for  $e_p^k$  and  $\vec{e}_{S\tau}^k$ . Hence we have proved the following theorem.

**Theorem 4** Assume  $\gamma_f < \gamma_p, \mathbb{K}$  is isotropic, and  $\alpha$  is small enough such that (5.35) is true. If  $\gamma_f$  and  $\gamma_p$  are close to each other such that (6.54) and (6.55) are true, then

$$\begin{aligned} \phi_D^k & \xrightarrow{X_D} \phi_D \quad \vec{u}_S^k \xrightarrow{X_S} \vec{u}_S \quad p_f^k \xrightarrow{Q_S} p_S, \\ \eta_p^k & \xrightarrow{L^2(\Gamma)} \gamma_p \vec{u}_S \cdot \vec{n}_S + g\phi_D = -\gamma_p \mathbb{K} \nabla \phi_D \cdot \vec{n}_D + g\phi_D, \\ \eta_f^k & \xrightarrow{L^2(\Gamma)} \gamma_f \vec{u}_S \cdot \vec{n}_S - g\phi_D = \vec{n}_S \cdot (\mathbb{T}(\vec{u}_S, p_S) \cdot \vec{n}_S) + \gamma_f \vec{u}_S \cdot \vec{n}_S, \\ \vec{\eta}_{f\tau}^k & \xrightarrow{H^{-\frac{1}{2}}(\Gamma)} \frac{\alpha v \sqrt{d}}{\sqrt{\text{trace}(\mathbb{I})}} P_\tau \mathbb{K} \nabla \phi_D. \end{aligned}$$

Specifically, if  $\gamma_f$  and  $\gamma_p$  are close to each other such that (6.56) and (6.57) are true, we then have the geometric convergence rate  $\sqrt{\frac{\gamma_f}{\gamma_p}}$ .

### 7 Computational examples

First we consider the model problem (2.1)–(2.7) on  $\Omega = [0, 1] \times [-0.25, 0.75]$  where  $\Omega_D = [0, 1] \times [0, 0.75]$  and  $\Omega_S = [0, 1] \times [-0.25, 0]$ . Choose  $\frac{\alpha v \sqrt{d}}{\sqrt{\text{trace}(\mathbb{I})}} = 1, \nu = 1, g = 1, z = 0$ , and  $\mathbb{K} = KI$  where  $I$  the identity matrix and  $K = 1$ . The boundary condition data functions and the source terms are chosen such that the exact solution of the Stokes–Darcy system with the BJ interface condition is given by

$$\begin{cases} \phi_D = [2 - \pi \sin(\pi x)][-y + \cos(\pi(1 - y))], \\ \vec{u}_S = [x^2 y^2 + e^{-y}, -\frac{2}{3} x y^3 + 2 - \pi \sin(\pi x)]^T, \\ p_S = -[2 - \pi \sin(\pi x)] \cos(2\pi y). \end{cases}$$

We use a uniform grid with grid size  $h$ . The Taylor–Hood element pair is used for the Stokes system and the quadratic finite element is used for the primary formulation of the Darcy system.

*Remark 2* In order to ensure the convergence of the proposed domain decomposition methods, the parameters  $\gamma_f$  and  $\gamma_p$  should be chosen carefully. One way is to choose

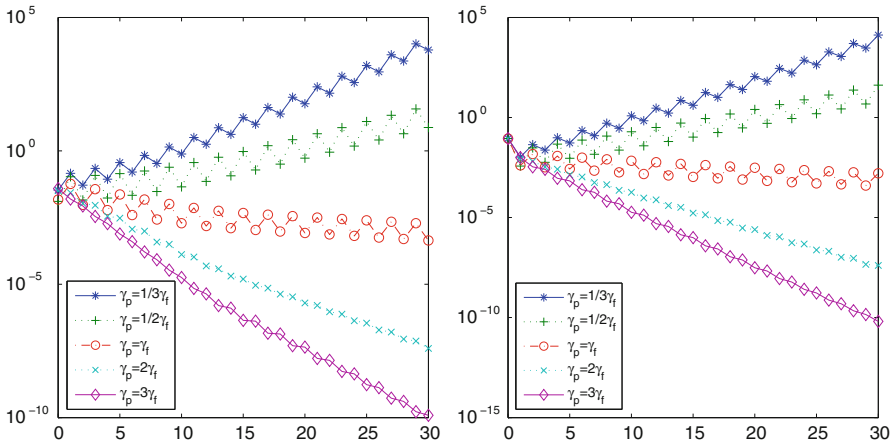


**Fig. 2**  $L^2$  errors in hydraulic head (left) and velocity (right) versus the iteration counter  $k$  for the parallel Robin–Robin domain decomposition method with  $\nu = 1$ ,  $K = 1$ ,  $\gamma_f = 1.5$ , and  $h = 1/32$

$\gamma_f = \gamma_p = \gamma$  for some  $\gamma$ . It works for practical coefficients, but the convergence may be slow, see Figs. 2–7. In order to obtain a better convergence rate, we need to use different  $\gamma_f$  and  $\gamma_p$ . If  $\gamma_f < \gamma_p$ , then they need to be chosen so that the sufficient conditions in Theorems 2 and 4 are satisfied. There are some discussions in detail with different numerical experiments for this issue in [25]. Here we will discuss how to choose  $\gamma_f$  and  $\gamma_p$  by using (5.42), (5.43) and the parameters given before. Note that  $C_1$  depends on  $\nu = 1$  and  $K = 1$  linearly and  $C_2$  depends on  $K = 1$  linearly. Hence they are of order 1. In addition, by the domain and interface chosen above,  $C_3$  and  $C_4$  are also of order 1. Therefore, the right-hand-side of (5.42) and (5.43) are of order 1. In the following we will see the convergent numerical results with  $\gamma_f = 1.5$  and  $\gamma_p = 1.5, 3, 4.5$ . More discussion about  $\gamma_p = \frac{1}{10}$  and  $\gamma_f = \frac{1}{10}, \frac{1}{20}, \frac{1}{30}$  can be found in [25]. As for the practical coefficients  $\nu = 10^{-6}$  and  $10^{-7} \leq k \leq 10^{-2}$  in the international system, the corresponding Stokes–Darcy model becomes more difficult to solve. Hence  $\gamma_f$  and  $\gamma_p$  may need to be chosen more carefully. The results in Figs. 6 and 7 suggest that we should choose  $\gamma_f > \gamma_p$ . But a more careful analysis needs to be carried out to provide more information and details about how to choose  $\gamma_f$  and  $\gamma_p$ . In order to overcome the difficulty of the Neumann–Dirichlet domain decomposition method [31,32] for realistic applications, [43] proposed an approach based on the recovery of the Neumann–Dirichlet iteration operator for the error. Meanwhile, as suggested in [43], the Robin–Robin domain decomposition method with two relaxation parameters in [28] is one alternative method for realistic scenarios. These lead to some interesting future work for Stokes–Darcy model with realistic parameters.

Figures 2 and 3 show the  $L^2$  errors of hydraulic head, velocity, pressure and  $\eta_f$  for the parallel DDM with  $\nu = 1$ ,  $K = 1$ ,  $\gamma_f = 1.5$ , and  $h = 1/32$ . We can see that the parallel domain decomposition method is convergent for  $\gamma_f \leq \gamma_p$ , which computationally verifies the conclusions given in Sect. 5.

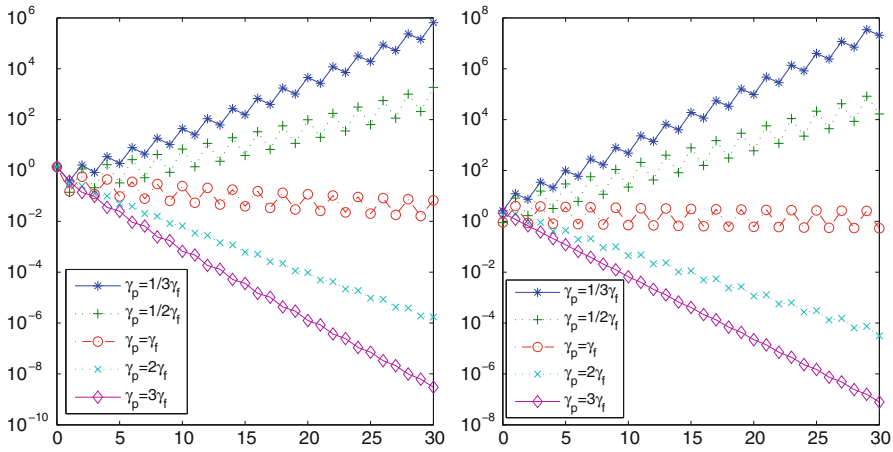


**Fig. 3**  $L^2$  errors in pressure (left) and  $\eta_f$  (right) versus the iteration counter  $k$  for the parallel Robin–Robin domain decomposition method with  $\nu = 1$ ,  $K = 1$ ,  $\gamma_f = 1.5$ , and  $h = 1/32$

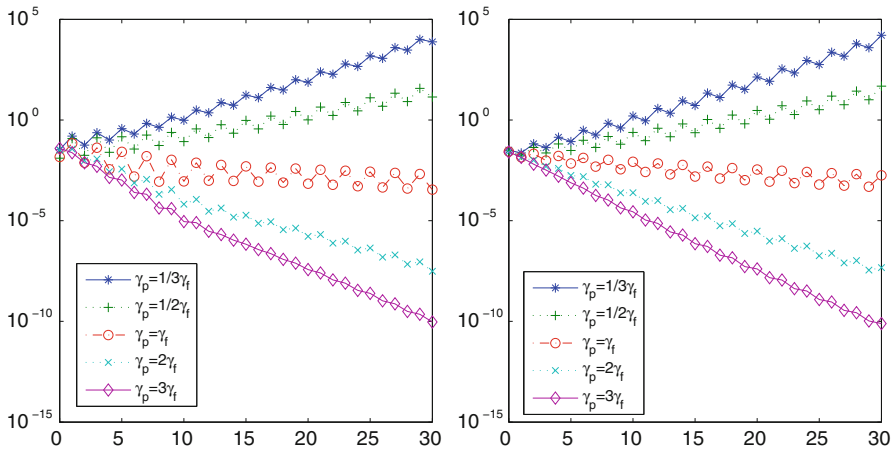


**Fig. 4**  $L^2$  errors in hydraulic head (left) and velocity (right) versus the iteration counter  $k$  for the serial Robin–Robin domain decomposition method with  $\nu = 1$ ,  $K = 1$ ,  $\gamma_f = 1.5$ , and  $h = 1/32$

Tables 1 and 2 list some  $L^2$  errors in hydraulic head, velocity, pressure and  $\eta_f$  for the parallel domain decomposition method with  $\nu = 1$ ,  $K = 1$ ,  $\gamma_f = 1.5$ ,  $\gamma_p = 4.5$ , and  $h = 1/32$ . Let  $e(i)$  denote the error at the  $i^{th}$  iteration step. We can see all the error ratios are less than  $\left(\sqrt{\frac{\gamma_f}{\gamma_p}}\right)^6 = \left(\sqrt{\frac{1}{3}}\right)^6 \approx 0.037$ , which numerically confirms the geometric convergence rate in Theorem 2.

Figures 4 and 5 show the  $L^2$  errors of hydraulic head, velocity, pressure and  $\eta_f$  for the serial domain decomposition method with  $\nu = 1$ ,  $K = 1$ ,  $\gamma_f = 1.5$ , and  $h = 1/32$ . We can see that the serial domain decomposition method is convergent for  $\gamma_f \leq \gamma_p$ , which computationally verifies the conclusions given in Sect. 6.

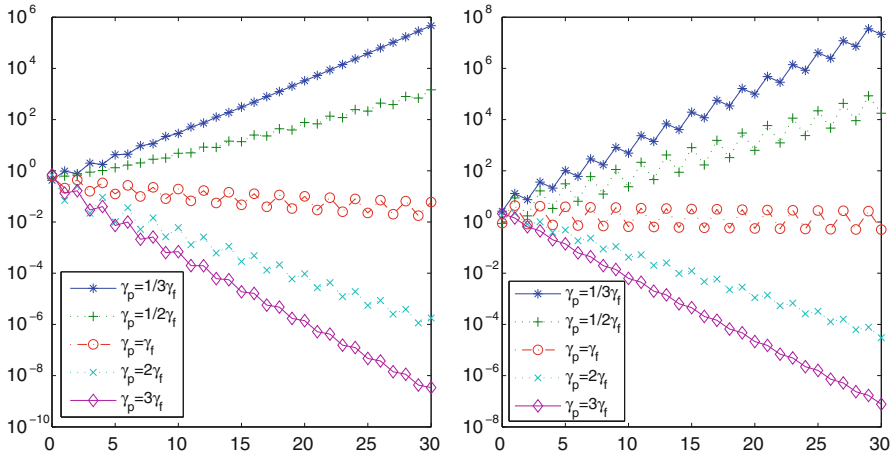


**Fig. 5**  $L^2$  errors in pressure (left) and  $\eta_f$  (right) versus the iteration counter  $k$  for the serial Robin–Robin domain decomposition method with  $\nu = 1$ ,  $K = 1$ ,  $\gamma_f = 1.5$ , and  $h = 1/32$

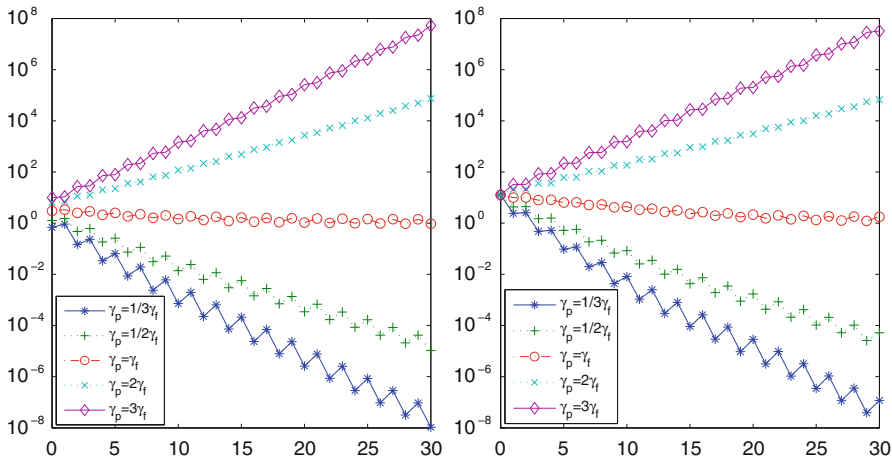


**Fig. 6**  $L^2$  hydraulic head (left) and velocity (right) errors of the iterates versus the iteration counter  $k$  for the parallel Robin–Robin domain decomposition method with  $\nu = 10^{-6}$ ,  $K = 10^{-6}$ ,  $\gamma_f = 1.5$ , and  $h = 1/32$

For the serial domain decomposition method, we observe very similar performance to Tables 1 and 2. Additionally, for both the parallel and serial methods, we have similar observations for the errors in other proper norms, including the errors of hydraulic head and velocity in  $H^1$  norm and discrete maximum norm and the errors of pressure and  $\eta_f$  in discrete maximum norm. Hence we omit the related plots and tables here to reduce the presentation.

Table 3 shows the number of iterations  $M$  for different grid sizes for both domain decomposition methods. Here, we set  $\gamma_f = 1.5$ ,  $\gamma_p = 3\gamma_f$ ,  $\nu = 1$ , and  $K = 1$ . Let  $\phi_h^k$ ,  $\vec{u}_h^k$  and  $p_h^k$  denote the finite element solutions of  $\phi_D^k$ ,  $\vec{u}_S^k$  and  $p_S^k$  at the  $k^{th}$  step



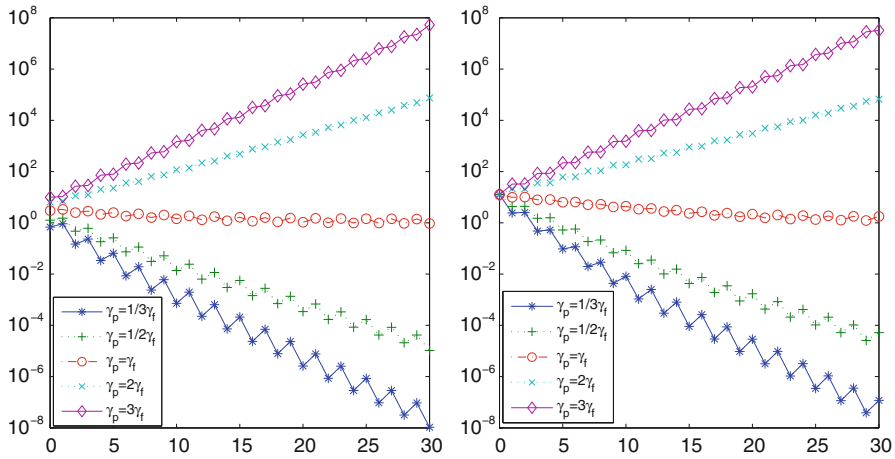


**Fig. 7**  $L^2$  hydraulic head (left) and velocity (right) errors of the iterates versus the iteration counter  $k$  for the serial Robin–Robin domain decomposition method with  $\nu = 10^{-6}$ ,  $K = 10^{-6}$ ,  $\gamma_f = 1.5$ , and  $h = 1/32$

**Table 1**  $L^2$  errors in hydraulic head and velocity for the parallel Robin–Robin domain decomposition methods

$h$	$L^2$ hydraulic head errors	$\frac{e(i)}{e(i-6)}$	$L^2$ velocity errors	$\frac{e(i)}{e(i-6)}$
$e(0)$	$3.8660 \times 10^{-2}$		$8.7996 \times 10^{-2}$	
$e(6)$ ( $i = 6$ )	$3.9456 \times 10^{-4}$	0.0107	$2.4444 \times 10^{-4}$	0.0028
$e(12)$ ( $i = 12$ )	$4.3271 \times 10^{-6}$	0.0110	$4.9673 \times 10^{-6}$	0.0203
$e(18)$ ( $i = 18$ )	$1.3567 \times 10^{-7}$	0.0314	$1.0885 \times 10^{-7}$	0.0219
$e(24)$ ( $i = 24$ )	$4.3338 \times 10^{-9}$	0.0319	$2.5597 \times 10^{-9}$	0.0237
$e(30)$ ( $i = 30$ )	$1.2128 \times 10^{-10}$	0.0280	$6.4020 \times 10^{-11}$	0.0250

**Table 2**  $L^2$  errors in pressure and  $\eta_f$  for the parallel Robin–Robin domain decomposition methods

$h$	$L^2$ pressure errors	$\frac{e(i)}{e(i-6)}$	$L^2$ errors in $\eta_f$	$\frac{e(i)}{e(i-6)}$
$e(0)$	$1.3845 \times 10^0$		$2.1170 \times 10^0$	
$e(6)$ ( $i = 6$ )	$9.2183 \times 10^{-3}$	0.0067	$6.6009 \times 10^{-2}$	0.0312
$e(12)$ ( $i = 12$ )	$1.8428 \times 10^{-4}$	0.0200	$2.1057 \times 10^{-3}$	0.0319
$e(18)$ ( $i = 18$ )	$4.2966 \times 10^{-6}$	0.0233	$6.8941 \times 10^{-5}$	0.0327
$e(24)$ ( $i = 24$ )	$1.1031 \times 10^{-7}$	0.0257	$2.3119 \times 10^{-6}$	0.0335
$e(30)$ ( $i = 30$ )	$3.0076 \times 10^{-9}$	0.0273	$7.9111 \times 10^{-8}$	0.0342

of the two proposed domain decomposition algorithms. The criteria used to stop the iteration, i.e., to determine the value  $M$ , is  $\|\vec{u}_h^k - \vec{u}_h^{k-1}\|_0 + \|\phi_h^k - \phi_h^{k-1}\|_0 + \|p_h^k - p_h^{k-1}\|_0 < \varepsilon$ , where the tolerance  $\varepsilon = 10^{-5}$ . We can see that the number of iteration steps  $M$  is independent of the grid size  $h$ .

**Table 3** The iteration counter  $K$  versus the grid size  $h$  for both the parallel and the serial Robin–Robin domain decomposition methods

$h$	$\frac{1}{8}$	$\frac{1}{16}$	$\frac{1}{32}$	$\frac{1}{64}$
$M$ for the parallel DDM	18	18	18	18
$M$ for the serial DDM	19	20	20	20

Practical coefficients  $\nu = 10^{-6}$  and  $10^{-7} \leq k \leq 10^{-2}$  in the international system may produce severe computational difficulties [43]. Therefore, in the following we present a numerical example with real world coefficients. We choose the same domains, boundary condition data functions, source terms and parameters as before, but  $\nu = 10^{-6}$  and  $K = 10^{-6}$ . From Figs. 6 and 7, we can see that the proposed domain decomposition methods are also applicable for real world coefficients with some proper choices of parameters  $\gamma_f$  and  $\gamma_p$ .

## 8 Conclusions

This article discusses two iterative domain decomposition methods, “parallel and serial”, for solving the steady Stokes–Darcy system with the Beavers–Joseph interface condition based on the two decoupled sub-problems. Both the analyses and numerical experiments demonstrate that the domain decomposition solutions converge to the solution of the coupled system and the geometric rate of convergence of the iterative schemes is confirmed. More extensive computational testing on more complicated geometries and with nonuniform meshes is underway. So far, most studies concerning domain decomposition methods for the Stokes–Darcy system address only the steady-state case. The domain decomposition method for the time-dependent Stokes–Darcy system is a subject of future research.

## References

1. Agoshkov, V.I.: Poincaré–Steklov operators and domain decomposition methods in finite dimensional spaces. In: First International Symposium on Domain Decomposition Methods for Partial Differential Equations (Paris, 1987), pp. 73–112. SIAM, Philadelphia (1988)
2. Agoshkov, V.I., Lebedev, V.I.: Poincaré–Steklov operators and methods of partition of the domain in variational problems. *Computat. Process. Syst.* **2**, 173–227 (in Russian) (1985)
3. Amara, M., Capatina, D., Lizaik, L.: Coupling of Darcy–Forchheimer and compressible Navier–Stokes equations with heat transfer. *SIAM J. Sci. Comput.* **31**(2), 1470–1499 (2008)
4. Arbogast, T., Brunson, D.S.: A computational method for approximating a Darcy–Stokes system governing a vuggy porous medium. *Comput. Geosci.* **11**(3), 207–218 (2007)
5. Arbogast, T., Gomez, M.: A discretization and multigrid solver for a Darcy–Stokes system of three dimensional vuggy porous media. *Comput. Geosci.* **13**(3), 331–348 (2009)
6. Babuška, I., Gatica, G.N.: A residual-based a posteriori error estimator for the Stokes–Darcy coupled problem. *SIAM J. Numer. Anal.* **48**(2), 498–523 (2010)
7. Badea, L., Discacciati, M., Quarteroni, A.: Numerical analysis of the Navier–Stokes/Darcy coupling. *Numer. Math.* **115**(2), 195–227 (2010)
8. Badia, S., Codina, R.: Unified stabilized finite element formulations for the Stokes and the Darcy problems. *SIAM J. Numer. Anal.* **47**(3), 1971–2000 (2009)
9. Beavers, G., Joseph, D.: Boundary conditions at a naturally permeable wall. *J. Fluid Mech.* **30**, 197–207 (1967)

10. Bernardi, C., Hecht, F., Nouri, F.Z.: A new finite-element discretization of the Stokes problem coupled with the Darcy equations. *IMA J. Numer. Anal.* **30**(1), 61–93 (2010)
11. Bernardi, C., Hecht, F., Pironneau, O.: Coupling Darcy and Stokes equations for porous media with cracks. *Math. Model. Numer. Anal.* **39**(1), 7–35 (2005)
12. Bernardi, C., Rebollo, T.C., Hecht, F., Mghazli, Z.: Mortar finite element discretization of a model coupling Darcy and Stokes equations. *Math. Model. Numer. Anal.* **42**(3), 375–410 (2008)
13. Boubendir, Y., Tlupova, S.: Stokes–Darcy boundary integral solutions using preconditioners. *J. Comput. Phys.* **228**(23), 8627–8641 (2009)
14. Bramble, J.H., Pasciak, J.E., Schatz, A.H.: The construction of preconditioners for elliptic problems by substructuring I. *Math. Comput.* **47**(175), 103–134 (1986)
15. Burman, E., Hansbo, P.: Stabilized Crouzeix–Raviart element for the Darcy–Stokes problem. *Numer. Methods Partial Differ. Equ.* **21**(5), 986–997 (2005)
16. Burman, E., Hansbo, P.: A unified stabilized method for Stokes’ and Darcy’s equations. *J. Comput. Appl. Math.* **198**(1), 35–51 (2007)
17. Cai, M., Mu, M., Xu, J.: Numerical solution to a mixed Navier–Stokes/Darcy model by the two-grid approach. *SIAM J. Numer. Anal.* **47**(5), 3325–3338 (2009)
18. Cai, M., Mu, M., Xu, J.: Preconditioning techniques for a mixed Stokes/Darcy model in porous media applications. *J. Comput. Appl. Math.* **233**(2), 346–355 (2009)
19. Cao, Y., Gunzburger, M., Hu, X., Hua, F., Wang, X., Zhao, W.: Finite element approximation for Stokes–Darcy flow with Beavers–Joseph interface conditions. *SIAM J. Numer. Anal.* **47**(6), 4239–4256 (2010)
20. Cao, Y., Gunzburger, M., Hua, F., Wang, X.: Coupled Stokes–Darcy model with Beavers–Joseph interface boundary condition. *Comm. Math. Sci.* **8**(1), 1–25 (2010)
21. Çesmelioglu, A., Rivière, B.: Analysis of time-dependent Navier–Stokes flow coupled with Darcy flow. *J. Numer. Math.* **16**(4), 249–280 (2008)
22. Çesmelioglu, A., Rivière, B.: Primal discontinuous Galerkin methods for time-dependent coupled surface and subsurface flow. *J. Sci. Comput.* **40**(1–3), 115–140 (2009)
23. Chen, N., Gunzburger, M., Wang, X.: Asymptotic analysis of the differences between the Stokes–Darcy system with different interface conditions and the Stokes–Brinkman system. *J. Math. Anal. Appl.* **368**(2), 658–676 (2010)
24. Chen, W., Chen, P., Gunzburger, M., Yan, N.: Superconvergence analysis of FEMs for the Stokes–Darcy system. *Math. Methods Appl. Sci.* **33**(13), 1605–1617 (2010)
25. Chen, W., Gunzburger, M., Hua, F., Wang, X.: A parallel Robin–Robin domain decomposition method for the Stokes–Darcy system. *SIAM J. Numer. Anal.* (to appear)
26. Chidyagwai, P., Rivière, R.B.: On the solution of the coupled Navier–Stokes and Darcy equations. *Comput. Methods Appl. Mech. Eng.* **198**(47–48), 3806–3820 (2009)
27. Dawson, C.: Analysis of discontinuous finite element methods for ground water/surface water coupling. *SIAM J. Numer. Anal.* **44**(4), 1375–1404 (2006)
28. Discacciati, M.: Domain decomposition methods for the coupling of surface and groundwater flows. PhD thesis, Ecole Polytechnique Fédérale de Lausanne, Switzerland (2004)
29. Discacciati, M.: Iterative methods for Stokes/Darcy coupling. In: *Domain Decomposition Methods in Science and Engineering. Lect. Notes Comput. Sci. Eng.*, vol. 40, pp. 563–570. Springer, Berlin (2005)
30. Discacciati, M., Miglio, E., Quarteroni, A.: Mathematical and numerical models for coupling surface and groundwater flows. *Appl. Numer. Math.* **43**(1–2), 57–74 (2002)
31. Discacciati, M., Quarteroni, A.: Analysis of a domain decomposition method for the coupling of Stokes and Darcy equations. In: *Numerical Mathematics and Advanced Applications*, pp. 3–20. Springer Italia, Milan (2003)
32. Discacciati, M., Quarteroni, A.: Convergence analysis of a subdomain iterative method for the finite element approximation of the coupling of Stokes and Darcy equations. *Comput. Vis. Sci.* **6**(2–3), 93–103 (2004)
33. Discacciati, M., Quarteroni, A., Valli, A.: Robin–Robin domain decomposition methods for the Stokes–Darcy coupling. *SIAM J. Numer. Anal.* **45**(3), 1246–1268 (2007)
34. Ervin, V.J., Jenkins, E.W., Sun, S.: Coupled generalized nonlinear Stokes flow with flow through a porous medium. *SIAM J. Numer. Anal.* **47**(2), 929–952 (2009)
35. Feng, M., Qi, R., Zhu, R., Ju, B.: Stabilized Crouzeix–Raviart element for the coupled Stokes and Darcy problem. *Appl. Math. Mech.* **31**(3), 393–404 (English Ed.) (2010)

36. Galvis, J., Sarkis, M.: Balancing domain decomposition methods for mortar coupling Stokes–Darcy systems. In: *Domain Decomposition Methods in Science and Engineering XVI*. Lect. Notes Comput. Sci. Eng., vol. 55, pp. 373–380. Springer, Berlin (2007)
37. Galvis, J., Sarkis, M.: Non-matching mortar discretization analysis for the coupling Stokes–Darcy equations. *Electron. Trans. Numer. Anal.* **26**, 350–384 (2007)
38. Galvis, J., Sarkis, M.: FETI and BDD preconditioners for Stokes–Mortar–Darcy systems. *Commun. Appl. Math. Comput. Sci.* **5**, 1–30 (2010)
39. Gander, M.: Optimized Schwarz methods. *SIAM J. Numer. Anal.* **44**(2), 699–731 (2006)
40. Gatica, G.N., Meddahi, S., Oyarzúa, R.: A conforming mixed finite-element method for the coupling of fluid flow with porous media flow. *IMA J. Numer. Anal.* **29**(1), 86–108 (2009)
41. Girault, V., Rivière, B.: DG approximation of coupled Navier–Stokes and Darcy equations by Beaver–Joseph–Saffman interface condition. *SIAM J. Numer. Anal.* **47**(3), 2052–2089 (2009)
42. Guest, J.K., Prévost, J.H.: Topology optimization of creeping fluid flows using a Darcy–Stokes finite element. *Int. J. Numer. Methods Eng.* **66**(3), 461–484 (2006)
43. Hoppe, R., Porta, P., Vassilevski, Y.: Computational issues related to iterative coupling of subsurface and channel flows. *CALCOLO* **44**(1), 1–20 (2007)
44. Hua, F.: Modeling, analysis and simulation of Stokes–Darcy system with Beavers–Joseph interface condition. Ph.D. dissertation, The Florida State University (2009)
45. Jäger, W., Mikelič, A.: On the interface boundary condition of Beavers, Joseph, and Saffman. *SIAM J. Appl. Math.* **60**(4), 1111–1127 (2000)
46. Jiang, B.: A parallel domain decomposition method for coupling of surface and groundwater flows. *Comput. Methods Appl. Mech. Eng.* **198**(9–12), 947–957 (2009)
47. Jones, I.: Low Reynolds number flow past a porous spherical shell. *Proc. Camb. Phil. Soc.* **73**, 231–238 (1973)
48. Kanschat, G., Rivière, B.: A strongly conservative finite element method for the coupling of Stokes and Darcy flow. *J. Comput. Phys.* **229**, 5933–5943 (2010)
49. Karper, T., Mardal, K.A., Winther, R.: Unified finite element discretizations of coupled Darcy–Stokes flow. *Numer. Methods Partial Differ. Equ.* **25**(2), 311–326 (2009)
50. Layton, W.J., Schieweck, F., Yotov, I.: Coupling fluid flow with porous media flow. *SIAM J. Numer. Anal.* **40**(6), 2195–2218 (2002)
51. Lions, P.-L.: On the Schwarz alternating method. III. A variant for nonoverlapping subdomains. In: *Third International Symposium on Domain Decomposition Methods for Partial Differential Equations* (Houston, TX, 1989), pp. 202–223. SIAM, Philadelphia (1990)
52. Mardal, K.A., Tai, X.C., Winther, R.: A robust finite element method for Darcy–Stokes flow. *SIAM J. Numer. Anal.* **40**(5), 1605–1631 (2002)
53. Masud, A.: A stabilized mixed finite element method for Darcy–Stokes flow. *Int. J. Numer. Methods Fluids* **54**(6–8), 665–681 (2007)
54. Mu, M., Xu, J.: A two-grid method of a mixed Stokes–Darcy model for coupling fluid flow with porous media flow. *SIAM J. Numer. Anal.* **45**(5), 1801–1813 (2007)
55. Nassehi, V., Petera, J.: A new least-squares finite element model for combined Navier–Stokes and darcy flows in geometrically complicated domains with solid and porous boundaries. *Int. J. Numer. Methods Eng.* **37**(9), 1609–1620 (1994)
56. Popov, P., Efendiev, Y., Qin, G.: Multiscale modeling and simulations of flows in naturally fractured karst reservoirs. *Commun. Comput. Phys.* **6**(1), 162–184 (2009)
57. Quarteroni, A., Valli, A.: Domain decomposition methods for partial differential equations. In: *Numerical Mathematics and Scientific Computation*. Oxford Science Publications, New York (1999)
58. Rivière, B.: Analysis of a discontinuous finite element method for the coupled Stokes and Darcy problems. *J. Sci. Comput.* **22**(23), 479–500 (2005)
59. Rivière, B., Yotov, I.: Locally conservative coupling of Stokes and Darcy flows. *SIAM J. Numer. Anal.* **42**(5), 1959–1977 (2005)
60. Rui, H., Zhang, R.: A unified stabilized mixed finite element method for coupling Stokes and Darcy flows. *Comput. Methods Appl. Mech. Eng.* **198**(33–36), 2692–2699 (2009)
61. Saffman, P.: On the boundary condition at the interface of a porous medium. *Stud. Appl. Math.* **1**, 77–84 (1971)
62. Salinger, A.G., Aris, R., Derby, J.J.: Finite element formulations for large-scale, coupled flows in adjacent porous and open fluid domains. *Int. J. Numer. Methods Fluids* **18**(12), 1185–1209 (1994)

63. Tai, X.C., Winther, R.: A discrete de Rham complex with enhanced smoothness. *CALCOLO* **43**(4), 287–306 (2006)
64. Tlupova, S., Cortez, R.: Boundary integral solutions of coupled Stokes and Darcy flows. *J. Comput. Phys.* **228**(1), 158–179 (2009)
65. Urquiza, J.M., N’Dri, D., Garon, A., Delfour, M.C.: Coupling Stokes and Darcy equations. *Appl. Numer. Math.* **58**(5), 525–538 (2008)
66. Xie, X., Xu, J., Xue, G.: Uniformly-stable finite element methods for Darcy-Stokes-Brinkman models. *J. Comput. Math.* **26**(3), 437–455 (2008)
67. Xu, J., Zou, J.: Some nonoverlapping domain decomposition methods. *SIAM Rev.* **40**(4), 857–914 (1998)
68. Xu, X., Zhang, S.: A new divergence-free interpolation operator with applications to the Darcy-Stokes-Brinkman equations. *SIAM J. Sci. Comput.* **32**(2), 855–874 (2010)
69. Zhang, S., Xie, X., Chen, Y.: Low order nonconforming rectangular finite element methods for Darcy-Stokes problems. *J. Comput. Math.* **27**(2–3), 400–424 (2009)